LOSS OF K_{ATP} CHANNEL ACTIVITY IN MOUSE FDB LEADS TO AN IMPAIRMENT IN ENERGY METABOLISM DURING FATIGUE

By

Kyle Scott

A thesis submitted to the Faculty of Graduate and Post-Doctoral Studies

of the University of Ottawa

in partial fulfillment of the requirements of the Degree of

Masters of Science

Department of Cellular and Molecular Medicine

Faculty of Medicine

University of Ottawa

ABSTRACT

Recently, it has been postulated that fatigue is a mechanism to protect the muscle fiber from deleterious ATP depletion and cell death. The ATP-sensitive potassium (K_{ATP}) channel is believed to play a major role in this mechanism. Under metabolic stress, the channels open, reducing membrane excitability, Ca^{2+} release and force production. This alleviates energy demand within the fiber, as activation of the channel reduces ATP consumption from cellular ATPases. Loss of K_{ATP} channel activity during fatigue results in excessive intracellular Ca^{2+} ($[Ca^{2+}]_i$) levels, likely entering the fiber through L-type Ca^{2+} channels. It has been demonstrated that when mouse muscle lacking functional K_{ATP} channels are stimulated to fatigue, ATP levels become significantly lower than wild type levels. Thus, it was hypothesized that a lack of K_{ATP} channel activity impairs energy metabolism, resulting in insufficient ATP production. The focus of work for this M.Sc. project was to test this hypothesis. Fatigue was elicited in Kir6.2$^{-/-}$ FDB muscles for three min followed by 15 min recovery. After 60 sec, a 2.6-fold greater glycogen breakdown was observed in Kir6.2$^{-/-}$ FDB compared to wild type FDB. However, this effect disappeared thereafter, as there were no longer any differences between wild type and Kir6.2$^{-/-}$ FDB in glycogen breakdown by 180 sec. Glucose oxidation after 60 sec was also greater in Kir6.2$^{-/-}$ FDB compared to wild type FDB. However, levels of oxidation failed to increase in Kir6.2$^{-/-}$ FDB from 60 to 180 sec. Calculated ATP production during the fatigue period was 2.7-times greater in Kir6.2$^{-/-}$ FDB, yet measured ATP levels during fatigue are much lower in Kir6.2$^{-/-}$ FDB compared to wild type FDB. Taken together, it appears that muscle energy metabolism is impaired in the absence K_{ATP} channel activity.

TABLE OF CONTENTS

LIST OF FIGURES

LIST OF ABBREVIATIONS

$[\ ]_i$	intracellular concentration
$[\ ]_e$	extracellular concentration
ºC	degrees Celsius
AK	adenylate kinase
ANOVA	analysis of variance
AP	action potential
AMP	adenosine monophosphate
AMPK	AMP-activate protein kinase
ADP	adenosine diphosphate
ATGL	adipose triglyceride lipase
ATP	adenosine-5'-triphosphate
Ca^{2+}	calcium ion
CCPA	2-,chloro-N6-cyclopentyladenosine
Cl^-	chloride ion
ClC-1	chloride channel
CN	cyanide
CO_2	carbon dioxide
DHPR	dihydropyridine receptor
EDL	extensor digitorum longus
E_m	resting membrane potential
ETC	electron transport chain
FDB	flexor digitorum brevis

FABP	fatty acid binding protein
$FADH_2$	flavin adenine dinucleotide
FFA	free fatty acid
GLUT	glucose transporter
H^+	hydrogen ion
HSL	hormone sensitive lipase
Hz	hertz
IMP	inosine monophosphate
IMTG	intramuscular triglyceride
K^+	potassium ion
K_{ATP} channel	ATP-sensitive K^+ channel
K_{ir}	inward-rectifying potassium channel
K_v	voltage-sensitive K^+ channel
LDH	lactate dehydrogenase
L.S.D.	least significant difference
MHC	myosin heavy chain
mM	millimolar
μM	micromolar
mL	milliliter
MGL	monoglyceride lipase
mV	millivolt
n	number of sample
Na^+	sodium ion

Na_v	voltage-sensitive sodium channel
NADH	nicotinamide adenine dinucleotide
N/cm^2	Newton per centimeter square
NMJ	neuromuscular junction
PCr	phosphocreatine
PDH	pyruvate dehydrogenase
PFK	phosphofructokinase
PHOS	glycogen phosphorylase
P_i	inorganic phosphate
PIP_2	Phosphatidylinositol 4,5-bisphosphate
RyR	ryanodine receptor
S.E.	standard error
SERCA	sarco/endoplasmic reticulum
SR	sarcoplasmic reticulum
t-test	student t-test
Tm	tropomyosin
TM	transmembrane
TMD	transmembrane domain
Tn	troponin
WT	wild type

ACKNOWLEDGEMENTS

Thank you to my supervisor, Dr. Jean-Marc Renaud, for your teaching, guidance and help over the past few years. I have learned a great deal under your supervision, and I've always enjoyed the humour in the lab. It has been a great learning experience. I would also like to thank my advisory committee, Drs. Jocelyn Côté and Mary-Ellen Harper for their excellent advice and guidance.

To all of people I've worked with in the lab and on the floor: thank you as well. So many hours were spent working in the lab, but it was great to have such friendly people around to get through the grind.

I am indebted to all of my friends, both back home and in Ottawa, for supporting me and for just being great people! To Brooke, thank you for being so supportive, so caring and so amazing. You have helped me get through the ups and downs, and you have always been there for me along the way. I owe you so much. Finally, thank you to my family for also being so supportive and loving. I am grateful for all you've done.

CHAPTER 1

INTRODUCTION

At rest, the metabolic rate of skeletal muscle is very low, but once active can increase 100-fold (Gibbs et al., 1987). Due to the intense energy-consuming work that must be performed during muscular activity, substantial ATP generation is required to meet the needs of a high metabolic rate. During all types of exercise, eventually the ATP demand exceeds that of ATP production. If muscle suffers large ATP depletion, there is potential for fiber damage and cell death. It is therefore crucial for the muscle to have the capacity to prevent large ATP depletion.

Recently, it has been proposed that muscle fatigue is a mechanism to prevent damaging ATP depletion. Fatigue has been defined as "a transient and recoverable decline in muscle force and/or power with repeated or continuous muscle contractions" (Mckenna et al., 2008). There are now several lines of evidence for intracellular components that behave as energy sensors that eventually trigger fatigue (Gong et al., 2003, Pedersen et al., 2009). One of them is the ATP-sensitive potassium (K_{ATP}) channel, which is found in many different tissues, including skeletal muscle. This ion channel links the energy status of the cell to membrane excitability. During any metabolic stress, such as fatigue or ischemia, K_{ATP} channels are activated to reduce membrane excitability. As a consequence of lower membrane excitability, less Ca^{2+} is released from the sarcoplasmic reticulum (SR), leading to a decrease in force (Noma, 1983; Cifelli et al., 2007).

Despite a large body of studies demonstrating the mechanisms by which K_{ATP} channels depress membrane excitability as well as the damage induced by excessive

increases in intracellular calcium ([Ca^{2+}]i), little is known about how K_{ATP} channels affect energy metabolism. Therefore, the objective of this study was to determine how the complete loss of K_{ATP} channel activity affects carbohydrate and energy metabolism during fatigue.

MUSCLE CONTRACTION

Muscle contraction is first initiated when an action potential is transmitted from an alpha-motor neuron at the neuromuscular junction (NMJ). The signal along the nerve fiber causes acetylcholine to be released from the synaptic button into the synaptic cleft, the space separating the nerve fiber from the muscle. Acetylcholine binds to nicotinic acetylcholine receptors on the motor end plate of the muscle, causing a reconfiguration of the receptor, opening a pore that allows influx of cations, mainly Na^+. The positive charge of the sodium ions causes a large depolarization of the cell membrane. Once the depolarization threshold is met, there is an "all-or-none" response, where voltage-sensitive sodium (Na_V) channels quickly open to generate an action potential.

An action potential can be separated into two phases: the depolarization phase and the repolarization phase. The depolarization phase is caused by influx of Na^+ through (Na_V) channels, which start to open at a membrane potential (E_m) of -60mV (Chahine et al, 1994). As Na^+ moves across the membrane, E_m is depolarized from its resting values of -80 mV to +30 mV. The repolarization phase during which E_m returns towards the resting potential is the result of two events. The first event is the inactivation of Na^+ channels that decreases the permeability of Na^+ across the membrane. The second event is the activation of voltage-sensitive potassium (K_V) channels. Opening of the K_V channels causes an outward current of K^+ that repolarizes the cell membrane back to -80 mV.

After an AP is generated, patches of surrounding Na_V channels open, allowing

that area of cell membrane to become depolarized, resulting in another AP. This is referred to as propagation. From the NMJ, APs propagate along the sarcolemma and down cell membrane invaginations called transverse tubules (t-tubules).

The t-tubules contain voltage-gated Ca^{2+} (Ca_V) channels, also known as dihydropyridine receptors (DHPR) and L-type Ca^{2+} channels. When the membrane potential is less than -50 mV, the DHPR undergoes a conformational change, which then interacts with the Ca^{2+} release channel of the sarcoplasmic reticulum (SR), the ryanodine receptor (RyR). It is now well established that in skeletal muscle, DHPR and RyR-1 have reciprocal interactions that result in Ca^{2+} release from the SR (Nakai et al., 1998; Tanabe et al., 1990). Once the concentration of intracellular calcium ($[Ca^{2+}]_i$) increases in the sarcoplasm, contraction is initiated.

The smallest unit of contraction is the sarcomere. Within a sarcomere are the thin and thick filaments. In the thin filaments are two regulatory components, troponin (Tn) and tropomyosin (Tm), and one of the two contractile proteins, actin. The thick filament contains myosin, which contains a head that interacts with actin. Tn and Tm act to regulate the contraction cycle. Tn is a trimer, composed of 3 subunits: TnI, TnT and TnC. TnI is an inhibitory subunit that prevents the interaction between myosin and actin while Tm blocks the myosin binding sites on actin. TnT binds Tm and it also anchors the troponin complex to the thin filament (Greaser et al., 1973; Jin and Chong, 2010). TnC acts as the Ca^{2+} sensor, having four binding sites. When Ca^{2+} binds to TnC it causes a conformational change, exposing a hydrophobic region, to which TnI then attaches. In doing so, TnI relieves its inhibitory segment on the actin filament, which then causes TnT-bound tropomyosin to change position. This frees the myosin binding site on actin and initiates the contraction (Slupsky et al., 1995; Houdusse et al., 1997; Mercier et al.,

2003; Vinogradova et al. 2005).

In the resting state, an ADP and P_i molecule are bound to the myosin head and the energy of ATP has been transferred to myosin. In that state, the myosin head is cocked into a high-energy conformation. When myosin-binding sites on actin are free of Tm, myosin binds to actin, forming a crossbridge (Gordon et al., 2000). The powerstroke is initiated upon the release of P_i, where myosin pulls actin towards the center of the sarcomere, resulting in contraction. ADP is then released and the powerstroke is completed with the addition of more force. A new ATP molecule can then bind the myosin head, causing the dissociation of myosin from actin, returning to a low-energy state. To relax, Ca^{2+} is actively pumped back into the SR (Tupling et al., 2011).

There are three major ATPases that function during muscular activity: i) the myosin-ATPase, which is responsible for muscle shortening and accounts for 70% of the ATP utilization during activity (Kushmerick et al., 1969); ii) the sarco/endoplasmic reticulum Ca^{2+}-ATPase (SERCA), which actively pumps Ca^{2+} back into the SR between contractions, allowing the muscle to relax. This ATPase accounts for ~25-30% of the ATP utilization (Wendt et al., 1973; Rall, 1985); iii) the Na^+/K^+-ATPase, which is responsible for maintaining the Na^+ and K^+ gradients for APs by pumping out 3 Na^+ for every 2 K^+ that it pumps back into the cell. This ATPase comprises the remaining ATP utilization during muscular activity.

SKELETAL MUSCLE FIBER TYPES

Fiber types have been defined by the myosin heavy chain (MHC) isoform in which they express. In general, different fiber types also display different contractile, metabolic and functional characteristics. Type I fibers, known as slow-twitch fibers, are characterized by slow contractile speeds, indicated through slow force development and

low shortening velocity (Bottinelli et al., 1991; Widrick et al., 1996). Type II fibers, known as fast-twitch fibers, are divided into three types: IIA, IIB, and IIX. Type II fibers have greater contractile speeds than Type 1 fibers, where the maximum shortening velocities follow the order IIB > IIX > IIA > I (Trappe et al., 2000; Widrick et al., 2001; Widrick, 2002)

In addition to defining fiber types based upon contractile characteristics, there are also fiber type-specific isoforms for troponin. These include slow and fast types in each of the troponin complex subunits. Soleus muscle, which is composed primarily of slow-twitch fibers contains the slow troponin isoforms, while extensor digitorum longus (EDL) muscle, which consists of IIB, IIX and IIA fibers, expresses the fast troponin forms (Parmacek et al., 1989; Parmacek et al., 1990; Brotto et al., 2006). Brotto et al. (2006) demonstrated that fast and slow troponin isoforms are correlated with lower and higher Ca^{2+} sensitivities, respectively. In EDL muscles, which expressed fast TnT/TnI, the Ca_{50} was 2.30 μM, while soleus muscles, expressing slow TnT/TnI had a Ca_{50} of 1.92 μM.

Furthermore, there are specific SERCA isoforms that characterize the different fiber types. Soleus muscle is composed of SERCA2a isoforms, which are also found in cardiac muscle, while SERCA1a is found in EDL muscle (Wu and Lytton, 1993). The two separate isoforms for fast- and slow-twitch muscle types are extremely important when muscle is active as the former requires rapid relaxation between contractions during activities such as sprinting, while the latter type is often used for posture.

Generally type I and IIA fibers express high oxidative capacities, with higher mitochondrial content, oxidative enzymes, myoglobin and blood vessels (Bonen et al., 1999). Consequently, they are highly fatigue resistant (Bonen et al., 1999). This is of great importance, considering type I fibers are activated mainly for posture, while IIA

fibers are relied upon heavily during prolonged exercise, such as endurance running. Contrastingly, type IIB fibers have the lowest mitochondrial content, yet have the highest glycolytic capacity, along with the highest glycogen content (Spriet, 1979; Dyck et al., 1997). They rely primarily on glycolysis to produce ATP and are the most fatiguable fibers. Type IIX fibers lay in between IIA and IIB fibers in terms of their oxidative and glycolytic capacities. Interestingly, rodents are known to express all four types of fibers, whereas humans only express I, IIA and IIX fibers.

ENERGY METABOLISM DURING EXERCISE

Endogenous ATP is the direct energy source used by all cellular ATPases. However, during muscle contraction, especially at high intensity, if this were the only source of ATP, its depletion would occur within seconds. In muscle, ATP rarely falls below 20 percent of resting levels (Spriet et al., 1985; Ren et al., 1990; Balsom et al., 1995; Sahlin and Harris 2011), consistent with the fact that skeletal muscle has a multitude of energy-providing pathways, which confers a tremendous capacity to meet energy needs so that performance can be sustained.

As mentioned previously, skeletal muscle can upregulate metabolic enzymes up to 100-fold at the onset of activity in order to match the large ATP requirement (Gibbs, 1987). As a consequence, there are increases in metabolic by-products and end-products, which vary based upon the intensity and duration of exercise. Metabolic pathways as well as studies concerning the change in metabolites during contraction and exercise in both rodent models and humans will now be discussed.

ATP

At rest, levels of ATP are in the range of 22 – 29 μmoles/g dry weight (Balsom et al., 1995; Chesley et al., 1998; Tsintzas et al., 2001; Gray et al., 2011). The breakdown of

ATP to produce energy for contraction is as follows:

$$ATP \rightarrow ADP + P_i + energy$$

It has been demonstrated from many human studies that ATP levels remain close to resting levels during many types of exercise. For example, Balsom et al. (1995) studied subjects sprinting on a cycle ergometer for periods of 6 sec, 5 times, with rest periods of 30 sec in between, followed by a 6th sprint 40 sec later lasting 10 sec. Despite the high-intensity protocol, resting ATP content was only 4.8 mmol/kg dry weight (or 21%) less after the 6th sprint when compared to pre-exercise levels. Similarly, Ren et al. (1990) demonstrated a decrease from 25 to 23.7 mmol/kg dry weight after 30 min of intense quadriceps femoris stimulation. Jones and colleagues (1985) showed no change in ATP levels of human subjects after 30 sec of high intensity cycling at 140 rpm, despite the initial power decreasing to less than half at the end of exercise. Finally, there was very little change in ATP after prolonged moderate-intensity exercise in subjects cycling for 77 min, where levels decreased from 24.4 mmol/kg dry weight to only 21.1 mmol/kg dry weight (Sahlin et al., 1997).

Studies of rodents have given similar results (Spriet, 1985; Ren et al., 1990; Ihlemann et al., 2000; Ortenblad et al., 2009). Even when blood flow was occluded to block oxygen and fuel sources to fast-twitch gastrocnemius muscle, ATP levels decreased only by 26% after 60 sec of contraction at a rate of one tetanus every 2 sec (Spriet et al., 1989). Albeit, 60 sec of contraction every sec did result in a 63% decrease in ATP. Thus, unless oxygen is low, ATP levels are maintained proficiently even during intense muscular activity.

Phosphocreatine

While the different energy pathways are not serially activated, the first to become upregulated is the phosphocreatine (PCr) reaction. PCr provides a high-energy phosphagen store, which, when catalyzed by creatine kinase, helps to maintain ATP levels constant at the onset of exercise until other ATP metabolic pathways are upregulated. Its breakdown is initiated by an increase in ADP (Sahlin and Harris 2011). The PCr reaction is as follows:

$$PCr + ADP + H^{+} \leftrightarrow Cr + ATP$$

The transfer of high-energy phosphates from PCr to free ADP provides ATP replenishment for the first 20 - 50 sec of muscular activity (Hultman et. al, 1983; Greenhaff et al, 1994; Li, 2007). Resting levels of PCr are greater in fast-twitch fibers compared to slow-twitch fibers, as seen in human vastus lateralis tissue where PCr content is approximately 80 mmol/kg dry mass in Type II fibers compared to 66 mmol/kg dry mass in Type I fibers (Tsintzas et al. 2001). This has been demonstrated in other studies as well (Kushmerik et al., 1992; Sahlin et al., 1997). Compared to Type I fibers, PCr utilization is also higher in Type II fibers. For example, when human subjects cycled until fatigue, PCr levels decreased by 64% in Type I fibers, while they decreased by 71% in Type II fibers (Sahlin et al., 1997). The extent to which PCr is degraded is dependent upon the intensity of exercise. For example, McCartney et al. (1986) demonstrated PCr levels decreased from 14.26 to 0.6 mmol/kg wet weight after four 30-sec cycling sprints. Large decreases in PCr during high-intensity exercise have been reported elsewhere (Sahlin et al., 1989; Gibala et al., 2009; Gray et al., 2011) In addition to the large decreases seen during high-intensity exercise, PCr stores are also hydrolyzed to a

significant extent during submaximal intensities. Sahlin and colleagues (1997) had subjects cycle for approximately 77 min at 75% of their VO_2 max, which is an estimate of the amount an individual's muscles can transport and use oxygen during exercise, and it also indicates exercise intensity. PCr levels had declined to 37% of resting levels, indicating that a large proportion of PCr stores can be broken down even at a moderate intensity.

During low-intensity exercise, there is less reliance upon PCr stores. After 10 min of low-intensity cycling, contents diminished by ~2%, thus relying very minimally upon PCr degradation (Campbell-O'Sullivan et al., 2002). These studies signify that skeletal muscle is reliant upon the degradation of PCr during moderate to high intensities, which is also when Type II fibers are predominantly activated, and that the effect of greater PCr utilization is to buffer ATP levels during the early stages of exercise. Prolonged muscular activity requires other mechanisms of provisioning ATP. Glycolysis is upregulated during the degradation of PCr, as its breakdown consumes a H^+. This leads to an increase in pH_i, decreasing the inhibition of the rate-limiting glycolytic enzyme, phosphofructokinase (PFK) (Meyer et al., 1986). Thus, as PCr is degraded, it allows flux through glycolysis to increase and provide more ATP for the working muscle.

Glycolysis

Energy provision by glycolysis is rapid, yet the abundance of ATP generated per glucosyl unit is only 2 or 3 ATP, depending on whether the glucosyl comes from extracellular glucose or from intracellular glycogen. Rates of glycolysis increase immensely with elevated intensity of exertion, especially in fast-twitch fibers (Campbell-O'Sullivan et al., 2002; Talanian et al., 2006). When glucose enters the cell, it is first phosphorylated by the ATP-dependent hexokinase (HK) to glucose-6-phosphate (G-6-P).

In this case, glycolysis yields 2 net ATP, as follows:

$$\text{G-6-P} + 2\ \text{ADP} + 2\ \text{NAD}^+ + 2\ \text{P}_i \rightarrow 2\ \text{Pyruvate} + 2\ \text{ATP} + 2\ \text{NADH} + 2\ \text{H}^+$$

Extracellular glucose is transported across the plasma membrane by glucose transporters (GLUTs). While GLUT1 is the main transporter of glucose into the muscle at rest, GLUT4 transports the majority of glucose across the sarcolemma during contraction (Etgen et al., 1993). A major regulator of GLUT4 translocation during contraction is Ca^{2+}. Furthermore, it is proposed that the role of Ca^{2+} in the recruitment of GLUT4 involves activation of calmodulin as well as protein kinase C (PKC) (Jensen et al., 2007; Thong et al., 2007; Wright et al., 2004; Wright et al., 2005). Another constituent in signaling the movement of transporters to the cell membrane is AMP-activated protein kinase (AMPK) (Holmes et al., 1999; Ojuka et al., 2002). AMPK is activated during metabolic stress, and one of the main activators is AMP (Ihlemann et al., 2000; Raney et al., 2008; McGee and Hargreaves, 2010). In a rodent study, there was a 30-40% decrease in contraction-stimulated glucose uptake in mouse EDL and soleus muscles when AMPK activity was abolished, suggesting that AMPK is required for partial stimulation of GLUT4 membrane recruitment, while other AMPK-independent pathways are needed for complete contraction-induced translocation, such as Ca^{2+} (Mu et al., 2001). Thus the action of GLUT4 translocation appears to be regulated by multiple pathways converging on intracellular GLUT4 storage areas to increase transporters at the sarcolemma and facilitate greater glucose uptake during muscular activity.

Within muscle, glucose is stored as glycogen. Glycogen is broken down by the enzyme glycogen phosphorylase (PHOS). Glucosyl units enter glycolysis as glucose-1-phosphate (G-1-P). Breakdown of G-1-P yields 3 ATP as it bypasses the hexokinase-

mediated phosphorylation of glucose to G-6-P. The reaction is as follows:

$$\text{G-1-P} + 3\ \text{ADP} + 2\ \text{NAD}^+ + 3\ \text{P}_i \rightarrow 2\ \text{Pyruvate} + 3\ \text{ATP} + 2\ \text{NADH} + 2\ \text{H}^+$$

There is increasing evidence that there are three subcellular pools of glycogen: intramyofibrillar, intermyofibrillar and subsarcolemmal. These appear to be specific for providing a fuel source to the cellular machinery located at those areas. The intramyofibrillar glycogen pool is located in the sarcomere between actin and myosin filaments (Nielsen et al., 2011). Being in close proximity to these contractile proteins, intramyofibrillar glycogen enables a rapid provision of phosphagens to myosin-ATPases to convert chemical energy into mechanical work (Friden et al., 1989). Both Type I and II fibers show preferential degradation of this source of glycogen (Nielsen et al., 2011). The second glycogen pool is the intermyofibrillar pool, located near both the SR as well as mitochondria. This pool is believed to be involved in Ca^{2+} reuptake between contractions and makes up 75% of total myofibrillar glycogen (Friden et al., 1989; Nielsen et al., 2009). The third pool is the subsarcolemmal glycogen pool, which is likely relied upon to maintain membrane excitability by providing ATP to the Na^+K^+-ATPase (Friden et al., 1985). This glycogen pool makes up 11 and 8% of total glycogen content in Type I and II fibers, respectively (Nielsen et al., 2011).

These different subcellular pools, specific to the ATP-consuming enzymes of the cell, confer advantages in terms of minimizing the diffusion distance of ATP to these enzymes. Although recent research has begun to investigate the different subcellular locations of glycogen and their respective roles during exercise, most studies have measured glycogen from muscle homogenates, measuring overall glycogen content from samples. These studies will now be discussed.

During low-intensity exercise, reliance upon glycogen is much lower than at high intensities. In one study, 30 min of cycling resulted in a 14% decrease in pre-exercise glycogen levels, decreasing further to 26% after 60 min (Nordheim et al., 1990). Similar decreases during low-intensity exercise have been demonstrated in other studies (Karlsson et al., 1970; Gollnick et al., 1974; Price et al., 1991). After subjects cycled for 30 min while performing a crank ergometer as well, glycogen content in triceps muscles decreased to 40% of initial resting stores (Kiilerich et al., 2008). In the case of exhaustive sprint exercise, glycogen becomes the main source of glucosyl units for glycolysis and its concentration can be reduced by 60 – 80% (Kiilerich et al., 2008; Graham et al., 2010; Green et al., 2011). Thus reliance upon intramuscular glycogen stores increases with the intensity and duration of exercise, providing glycolysis with substrate to generate energy for the increased demand.

The major end product of glycolysis is pyruvate, and it has two possible fates. One is its conversion by pyruvate dehydrogenase (PDH) to acetyl-coenzyme A (acetyl-CoA), which then enters the Krebs cycle to become oxidized. The other fate occurs when pyruvate accumulates faster than the rate at which PDH can convert it to acetyl-CoA. When this happens, pyruvate is converted by lactate dehydrogenase (LDH) to lactate and NAD^+.

At rest, muscle lactate production is minimal, being approximately 3-6 mmol/kg dry mass (Howlett et al., 1998; Gray et al., 2011; Wall et al. 2011). However, lactate accumulates early in exercise (Hultman and Sjoholm, 1983) and its production increases with exercise intensity (Babij et al., 1983). After 10 min of cycling at low intensity, lactate accumulation was minimal (4.7 mmol/kg dry muscle) compared to moderate intensity cycling where lactate accumulated to 37.5 mmol/kg dry muscle (Howlett et al.

1998). At high-intensity, lactate content was even greater, reaching 107.9 mmol/kg dry muscle. These values have been confirmed by others (Sahlin et al., 1989; Bangsbo et al., 1994; Odland et al., 1998). Glycolytic fast-twitch muscles such as white gastrocnemius or EDL have greater accumulation of lactate compared to slow-twitch oxidative muscle such as soleus (Spriet et al., 1990). Correlated to increases in lactate during muscular stress, there is also a drop in intracellular pH (pH_i) (Welsh and Lindinger, 1997; Hollidge-Horvat et al., 1999) which may become as low as ~6.5 during intense activity (Hultman and Sjoholm, 1983).

Although anaerobic glycolysis followed by the production of lactate generates ATP at a rapid rate, glycogen as well as the rate of glycolysis can become limiting for ATP production. Thus another pathway, termed oxidative phosphorylation, generates ATP to a greater extent, albeit at a relatively slower rate compared to glycolysis. The products of glycolysis drive oxidative phosphorylation, being pyruvate as well as NADH and $FADH_2$, which are otherwise known as reducing equivalents.

Oxidative phosphorylation (OXPHOS)

Oxidative phosphorylation is the generation of ATP via the Electron Transport Chain (ETC), which is a series of complexes (I-IV), generating a H^+ gradient that drives the production of ATP. When pyruvate is converted to acetyl-CoA, the latter is combined with oxaloacetate to form citrate. This is the start of the Krebs Cycle, a series of enzymes that generate reducing equivalents, which act as substrates for the ETC. From one glucose molecule, ATP production through oxidative phosphorylation is as follows:

$$\text{Glucose} + 36\ \text{ADP} + 36\ P_i + 6\ O_2 \rightarrow 6\ CO_2 + 6\ H_2O + 36\ \text{ATP}$$

Another source of fuel for energy production is free fatty acids (FFAs). FFAs are carbon

chains that are first broken down to 2 carbon molecules (ie. acetyl-CoA). The pathway is termed β-oxidation, as it is the β position at which the FFA is cleaved to yield an acetyl-CoA molecule. The reaction is as follows:

$FFA(n) + nATP + nCoA + nFAD \rightarrow nAcetyl\text{-}CoA + 2nP_i + nAMP + nNADH + nFADH_2$,

where n represents the number of cleavages during β-oxidation. As described, the reducing equivalents produced during ß-oxidation of fatty acids are substrates for the ETC, by a series of REDOX reactions, generating ATP within the mitochondrion. For each NADH produced, there are 2.5 ATP produced, where for $FADH_2$ there are 1.5 ATP. Palmitic acid, a 16-carbon FFA molecule, would therefore produce 106 ATP if completely oxidized. Considering this, the ATP production per carbon molecule is greater for fat oxidation (6.6 ATP) compared to carbohydrate oxidation (6 ATP).

Similar to glucose metabolism, there are two sources of lipids for breakdown. One source involves the mobilization of FFA from adipose tissue. It is now thought that the mobilization of lipids is a process involving three main enzymes: adipose triglyceride lipase (ATGL), hormone sensitive lipase (HSL), and monoglyceride lipase (MGL) (Frederickson et al., 1981; Zimmermann et al., 2004; Watt et al., 2010). These liberate FFA from lipid droplets within adipose tissue into the blood where they can be taken up by muscle by the fatty acid transporters FAT/CD36 and FABP for subsequent oxidation or esterification. The other source for lipids resides within the muscle and is termed intramuscular triglycerides (IMTGs). Stores are greater in type I fibers compared to type II fibers (Essen, 1977), which is consistent with the greater oxidative capacity in these fibers (Bonen et al., 1999).

The contribution of fat oxidation for energy production was measured in a study

by Romijn and colleagues (1993) where cyclists performed for 2 hours on a stationary ergometer at three different intensities (25, 65 and 85% VO_2 max) each on separate days. After 30 min, the rate of fat oxidation increased from 25 to 65% VO_2 max and was 27 and 43 μmol/kg/min, respectively. However, at 85% the rate was actually lower, being 30 μmol/kg/min. The percent contribution of all energy sources also varied with intensity. At 25% VO_2 max, fatty acid oxidation accounted for approximately half of the energy expenditure, with the contribution of extracellular FFAs and IMTGs being equal. The contribution of total fat oxidation increased to 60% towards the end of the two hour ride, with the majority of FFAs coming from the blood. There was a much greater percent contribution of oxidation at 65% VO_2 max. During the two hour ride, 80 – 90% of the energy expenditure was from fat oxidation, with very little coming from IMTG stores.

Based on these findings, the contribution of fatty acids for energy production seems to increase from low to moderate activity, but is relied upon much less at higher intensities. This is consistent with the fact that the greater ATP demand at high-frequency contraction is met mainly by the more rapid glycolytic breakdown of glucose.

Adenine Nucleotides (ADP/AMP/IMP)

During extremely intense exercise, there is an increase in mismatch between ATP demand and production. ATP hydrolysis increases, resulting in a decreased ATP:ADP ratio. Since ADP is a substrate for ATP synthesis, which is a near-equilibrium reaction, a decreased ATP:ADP ratio could result in catastrophic energy depletion (Hancock et al., 2006). However, skeletal muscle has an intrinsic ability to prevent this. The adenylate kinase (AK) and AMP deaminase reactions prevent excessive accumulation of ADP, while producing further ATP for muscular activity. AK catalyzes the transfer of 1 molecule of inorganic phosphate (P_i) from one ADP to another resulting in ATP and

AMP. The reaction is as follows:

$$2\ ADP \leftrightarrow ATP + AMP$$

Since AK is a near-equilibrium enzyme, ensuring the reaction moves in the forward direction is crucial. Therefore, AMP deaminase is upregulated to cause a decrease in AMP, thus favouring the formation of ATP (above), with the reaction being:

$$AMP + H_2O \rightarrow IMP + NH_3$$

Concurrent with the increased utilization of ATP during exercise, there are also changes in the resultant adenine nucleotides: ADP, AMP and IMP (Spriet et al., 1987; Spriet et al., 1989). Changes in ADP and AMP are not drastic, but do increase during exercise (Krause et al., 1996; Febbraio et al., 1999). Sahlin and colleagues (1989) had subjects cycle at 40 and 70% VO_2 max for 10 min. ADP content rose to only 3.56 from 3.12 mmol/kg dry weight in the latter intensity exercise. In both cases, AMP increased from 0.09 mmol/kg dry weight to only 0.10 mmol/kg dry weight, while ATP levels decreased from 26.1 to 25.2 and 24.9 mmol/kg dry weight. At 100% VO_2 max, ADP and AMP rose to only 3.80 and 0.15 mmol/kg dry weight, respectively. So, the changes in these adenine nucleotides do not increase to a large extent. However at 100% VO_2 max IMP increased from <0.01 to 3.50 mmol/kg dry weight, reflecting a significant increase in activity of AMP deaminase. In another study, levels of IMP increased from 0.10 mmol/kg dry mass at rest to 6.40 mmol/kg dry mass after 30 sec of sprint cycling in human subjects (Zhao et al., 2000). The increase in IMP was proportional to the decrease in total adenine nucleotides. Overall, when ATP turnover is high, metabolic enzymes are capable of dealing with large perturbations in energy demand that could otherwise be threatening to the cell.

Based on the findings from studies done on both rodents and humans, it is clear

that there are changes in metabolites during muscular activity and the extent of these changes are dependent on the intensity of contraction. For a long time it was believed that the accumulation of metabolites during exercise was responsible for the decrease in force at the level of the sarcomere. However, as discussed below, more recent evidence from studies using higher, more physiological temperatures support the current belief that the role of metabolites on the decrease in force production is much smaller.

FATIGUE

Fatigue is defined as "a transient and recoverable decline in muscle force and/or power with repeated or continuous muscle contractions" (Mckenna et al., 2008). Decreases in the force production are anywhere from 50 – 80% of pre-fatigue values depending on the number of contractions and the duration of the contraction period (Westerblad et al., 1991; Cifelli et al., 2007; Cifelli et al., 2008). There are many levels at which fatigue is regulated, including central and peripheral fatigue. Central fatigue involves the central nervous system that decreases the drive of motor neurons, causing tremor in the working muscles and determines the perception of exertion (Gandevia, 1998). The idea of central fatigue is, however, controversial, as it has been suggested that its role in fatigue may be relatively minor (MacIntosh, 2011). Peripheral fatigue is the process occurring within skeletal muscle. It is now believed that fatigue is a mechanism to prevent detrimental effects to myocytes caused by deleterious ATP depletion (Kane et al., 2004; Thabet et al., 2005). The following discussion will be about the mechanisms of peripheral fatigue.

Role of metabolites in fatigue

For several years, researchers suggested that metabolites produced during contraction played a large part in eliciting fatigue by acting directly on the sarcomere.

These metabolites mainly include adenine nucleotides, IMP, P_i, H^+ and lactate. Although alterations in ATP, ADP and AMP during contraction were postulated to play a significant role in decreasing force production at the sarcomere, Godt and Nosek (1989) demonstrated that this was not the case. ATP was decreased to levels similar to that of fatigue and ischemia, from 6.18 to 4.7 mM. In contrast to previous beliefs, maximal force production (F_{max}) was not affected by low ATP as it was 99.7% of control force. Furthermore, low ATP resulted in an increase in Ca^{2+} sensitivity. ADP and AMP were also elevated to mimick situations of metabolic stress and these also increased F_{max} by 6 and 7% and did not decrease Ca^{2+} sensitivity. In addition, IMP, which increases from 0 to 5 mM during fatigue had no effect on force production or contractile speed during conditions mimicking low- and high-intensity muscular activity (Myburgh et al., 1997). This suggests that adenine nucleotides and IMP do not play a significant role during the fatigue process.

P_i increases as a result of PCr and ATP hydrolysis and can reach 30 mM during exercise (Sugaya et al., 2011). This has sparked much debate as to whether its accumulation has negative effects on the contractile machinery during fatigue (Kentish, 1986; Cooke et al., 1988; Godt and Nosek, 1989; Debold et al. 2006). A study by Kentish (1986) demonstrated that increasing muscle fiber P_i levels to 20 mM at room temperature increases Ca_{50} (the concentration of Ca^{2+} required to elicit half-maximal force) from 8.3 to 19.8 μM, signifying a 139% decrease in Ca^{2+} sensitivity. However, at 30ºC, the effects of P_i on calcium sensitivity are reduced in both slow type I and fast type II fibers (Debold et al., 2006).

Decreasing the pH from 7.0 to 6.0 resulted in a 46% decrease in isometric force in isolated rabbit psoas muscles, leading Cooke and colleagues (1988) to suggest that an

increase in H^+ ions during contraction plays a significant role in fatigue. In addition, decreasing pH from 7.0 to 6.2 resulted in a linear decrease in maximal force production to as low as 50% of the force seen at pH 7.0 (Godt and Nosek, 1989). Yet, at more physiological temperatures (32ºC), acidification of mouse FDB fibers caused no significant change in tetanic force compared to controls (Bruton et al., 1998). Furthermore, at 32ºC there was only a 10% decrease in tetanic force during intracellular acidification, compared to a 32% decrease at 12ºC. Pate and colleagues (1995) investigated the effect of decreased pH on contractile kinetics at low (10ºC) and near-physiological (30ºC) temperatures. Increasing temperatures to 30ºC at pH 6.2 abolished the decrease in shortening velocity, which was initially found to be a 30% decrease when experiments were performed at low temperature. The reduction in F_{max} also decreased by a factor of three when temperatures were elevated to 30ºC.

Andrews and colleagues (1996) demonstrated that increasing lactate concentrations within physiological ranges (0-25 mM) at pH 7 resulted in a decrease in maximal force production in chemically-skinned rabbit fast-twitch psoas fibers. However, this effect was not seen in slow-twitch, nor cardiac papillary muscles. The effect of lactate on force depression was not due to a decrease in Ca^{2+} sensitivity, as the force-pCa curves were not affected to a significant extent in any of the fiber-types. However, the decrease in force as a result of increased lactate concentration was quite small, being ~8%.

Overall, direct effects of metabolites on the sarcomere are either contrary to expectation or have an effect that is too small to largely contribute to the decrease in force at the level of the sarcomere. Thus, the mechanism causing a decrease in force during fatigue must be upstream. There is now a large body of evidence that clearly demonstrates that the amount of Ca^{2+} release by the SR decreases during fatigue to the

point that it is no longer fully activating the sarcomere; i.e. the [Ca^{2+}] during contraction becomes submaximal (Allen et al., 1989; Bruton et al., 1998; Lunde et al., 2001). Furthermore, Westerblad and Allen (1991) demonstrated that in the last phase of fatigue, the addition of 10mM caffeine blunted the 2-fold decline in force production and force became comparable to pre-fatigue force. Caffeine causes greater release of Ca^{2+} from the SR into the myoplasm, allowing [Ca^{2+}] to reach levels to fully activate the sarcomere. These results suggest: i) SR still have enough Ca^{2+} that, if released, can fully activate the sarcomere, and more importantly ii) if enough Ca^{2+} is released, the sarcomere is capable of developing as much force during fatigue than before fatigue is elicited, indicating the mechanism of fatigue is upstream of the sarcomere.

Possible mechanisms for decreased Ca^{2+} release

One of the mechanisms for decreased Ca^{2+} release may be the loss of glycogen stores during fatigue. When glycogen levels were decreased to 27% of resting values in mouse FDB bundles, myoplasmic Ca^{2+} during contraction and force decreased much more rapidly during fatigue when compared to the changes with normal glycogen levels (Chin and Allen, 1997).

Another explanation for the decrease in Ca^{2+} release during fatigue is at the level of membrane excitability. A link between energy metabolism and membrane excitability has recently been demonstrated (Ortenblad and Stephenson, 2003). When mitochondrial function was inhibited in terms of ATP generation, while maintaining intracellular ATP levels constant, twitch force was markedly reduced up to 90% when t-tubules were electrically stimulated. However, force was unaffected if t-tubules were completely depolarized by changing $[K^+]_e$. This suggests that while a membrane depolarization still triggers Ca^{2+} release, t-tubules are unable to generate action potentials. The authors had

suggested that the loss of membrane excitability was due to the release of a mitochondrial factor (yet to be identified) that eventually inhibits action potential generation in t-tubules.

There are also two ion channels in cell membranes that are ATP-dependent. The first is the chloride channel, CLC-1 (Bennetts et al., 2005; Bennetts et al., 2007). Activation of CLC-1 channels cause repolarization of the membrane and can also reduce the capacity to generate action potentials when $[K^+]_e$ is elevated during fatigue. There is now clear evidence for the activation of the CLC-1 channels during fatigue or during metabolic stress (Pedersen et al., 2005; Pedersen et al., 2009). The second channel is the ATP-sensitive potassium (K_{ATP}) channel, which is the focus of study in this thesis.

THE K_{ATP} CHANNEL

The ATP-sensitive (K_{ATP}) channels are weak inward rectifying channels that were first discovered in cardiac cells, where 1 mM ATP was sufficient to fully reduce the open probability of the channel to zero (Noma, 1983). The channel consists of two subunits (Kir and SUR) forming the pore and regulatory subunits, respectively. K_{ATP} channels are found throughout several tissues, including skeletal muscle (Spruce et al., 1985), pancreas (Cook et al., 1984), kidney (Meisheri et al., 1995) and brain (Murphy et al., 1990). The channel functions in glucose homeostasis and cytoprotection during metabolic stress.

Structure of the channel

Kir subunit

The K_{ir} subunit of the K_{ATP} channel is a member of the superfamily of inward rectifying channels, which consists of Kir1-Kir7 (Nichols and Lopatin, 1997; Aguilar-Bryan et al., 1999). In mammals, K_{ATP} channels are composed of Kir6 isoforms, which are further made up of two subsets: Kir6.1 and Kir6.2 and are encoded by genes KCNJ8 and KCNJ11, respectively (Inagaki et al., 1996; Flagg et al., 2010). The Kir subunits

comprise the pore of the channel, as K_{ATP} channels with truncated Kir6.2 proteins form functional channels independent of SUR subunit presence (Tucker et al., 1997). In contrast to voltage-sensitive (K_V) channels, Kir subunits contain two transmembrane domains, TM1 and TM2, with a hairpin loop between them, conferring the K^+ selectivity (Aguilar-Bryan et al. 1999). Specifically, there are highly conserved regions that are found in all K^+ channels allowing for K^+ specificity, that being TVGY/FG, otherwise known as the K^+ channel signature sequence. In addition, the NH_2 and COOH terminal regions interact to form the ATP-binding pocket that causes the closure of the channels (Flagg et al., 2010).

The C-terminal region contains an endoplasmic reticulum retention sequence, which, when truncated, gives rise to a functional channel (Tucker et al., 1997). The fact that 1 mM ATP reduced the channel activity in the absence of the SUR subunit, provided the first evidence that the inhibitory ATP-binding site resides on the Kir subunit. Later studies demonstrated that the phosphate of ATP binds the C-terminus in one subunit at positions R201 and K185 as well the N-terminus of another subunit at residue R50 (Tucker et al., 1998). Furthermore, the N6 atom of the adenine ring has an interaction with the same subunit at positions E179 and R301 (Antcliff et al., 2005).

SUR subunit

Sulfonylurea receptor (SUR) subunits belong to the ATP-binding cassette (ABC) superfamily. For K_{ATP} channels, two isoforms, SUR1 and SUR2 have been found. The gene ABCC8 encodes the SUR1 isoform, while SUR2 is encoded by ABCC9. Alternative splicing gives rise to SUR2A and SUR2B, which are expressed in different tissues with distinct properties (Aguilar-Bryan et al., 1995; Inagaki et al., 1995; Chutkow et al., 1996). There are 2 transmembrane domains (TMD1 and TMD2) for the SUR subunit, and each

of these contains six transmembrane helices in addition to large cytoplasmic domains containing regions for binding nucleotides. These nucleotide binding domains (NBDs) have both Walker A and B motifs which hydrolyze ATP to ADP, and are important for channel regulation (Walker et al., 1982; Aguilar-Bryan et al., 1999). SUR proteins are distinguished from the rest of the ABC superfamily by an additional domain (TMD0), which is joined to TMD1 in the cytosol. Its NH_2-terminus interacts with TMD0, which is important for the gating properties of the SUR subunit (Babenko and Bryan, 2003).

Electrophysiological properties of the Kir6.2 isoform of the K_{ATP} channel

Noma (1983) first observed that exposing cardiac cells to 5.4 mM cyanide (CN) to stop ATP production resulted in a large increase in membrane outward current that could be blocked with 1mM ATP. Resting ATP levels in human muscle is 5-7 mM (Spriet, 1991) and K_i of ATP is 17 μM (Davies et al., 1997). This suggests that during resting conditions the K_{ATP} channels are closed. Indeed, this is the case for isolated muscles (Spruce et al., 1985). However, using human subjects Nielsen et al. (2003) revealed that locally exposing muscle K_{ATP} channels with glibenclamide for 30 min reduced interstitial potassium from 4.5 to 4.0 mM. After 20 min of glibenclamide washout, levels of interstitial K^+ returned to initial levels. This suggests that at rest channels are activated *in vivo* and that ATP is not the only regulator of the channel. An answer for the discrepancy may be insulin. Exposing isolated muscle to insulin causes a hyperpolarization of resting E_m from -76 mV to -92 mV as the K_{ATP} channel opens, suggesting that some exogenous factors can activate the K_{ATP} channel even at mM ATP (Tricarico et al., 1999).

There is also evidence that K_{ATP} channels are activated during fatigue (Thabet et al., 2005; Cifelli et al., 2007; Pedersen et al., 2009). Therefore there must be other substrates responsible for overcoming the inhibition of K_{ATP} channels by ATP.

The SUR subunit is regulated by Mg nucleotides such that Mg-ADP results in channel opening, as does the binding and hydrolysis of Mg-ATP (Lederer and Nichols, 1989; Nichols, 2006). It appears that both nucleotide binding folds (NBFs) 1 and 2 are important for ADP-dependent opening of the channel. This is because mutations in NBF 1 at position G827 result in decreased channel activity, while mutations in the conserved lysine residues of NBF 2 prevent channel current (Shyng et al., 1997). Thus any increase in ADP during fatigue or any metabolic stress is expected to contribute to the activation of K_{ATP} channels.

Decrease in pH_i during fatigue is well documented (Howlett et al., 1998; Gorostioga et al., 2010) leading to channel activation (Davies et al., 1992; Standen et al., 1992). Acidifying frog muscle fibers from 7.19 to 6.45, which mimics decreases seen during intense exercise (Howlett et. al, 1998), caused approximately a 2-fold increase in K^+ current that can be blocked by glibenclamide, a K_{ATP} channel blocker. Moreover, similar decreases in pH_i increased the K_i for ATP from 17 to 260 μM (Davies et al., 1992). It appears that H^+ act mechanistically at 3 regions of the Kir6.2 subunit, being positions Thr71, Cys166 and His175 of the N-terminus, M2 and C-terminus regions, respectively (Piao et al., 2001). The significance of these studies is reflected by the fact that in the presence of these modulators, K_{ATP} channel activity is increased despite high levels of ATP.

Studies of cardiac cells have demonstrated that lactate may also regulate K_{ATP} channel activity (Keung and Li, 1991; Coetzee, 1992; Han et al., 1993). At concentrations of 20 and 40 mM, K_{ATP} channels were activated at ATP concentrations of 2 to 5 mM (Keung and Li, 1991). Although they did not directly test the mechanisms for lactate-induced activation of K_{ATP} channels, the authors suggested a few possibilities: 1) lactate

accumulation may lead to decreased ATP generation by glycolysis and thus decrease the ATP content; 2) sensitivity of ATP-sensing by K_{ATP} channels as a result of increased lactate; 3) lactate may act on the regulatory subunits to cause a conformational change in the channel, causing it to open; and 4) lactate may rely on interaction with other cellular components to cause K_{ATP} channels to open.

Finally, adenosine is a known metabolite, generated from ATP hydrolysis, which increases on the extracellular side of the membrane during any metabolic stress. Adding 100 μM adenosine increases K_{ATP} channel activity 100-fold (Barrett-Jolley et al., 1996). The study also showed that the activation involved an interaction between the A_1 receptor and a G-protein, interacting directly with the channel.

While it is not fully clear as to how the ATP inhibition of K_{ATP} channel is removed while ATP is still in the mM range, there is now clear evidence that the channels are activated during fatigue and that the decrease in pH, the increase in lactate as well as adenosine may be important factors.

Physiological roles of the K_{ATP} channel

The K_{ATP} channel is expressed throughout many tissues in the body. Two major functions for the K_{ATP} channel have been studied extensively; i.e. glucose homeostasis and cytoprotection.

Glucose homeostasis

K_{ATP} channels are involved in glucose homeostasis in a variety of tissues, which include the α and β cells of the pancreas, neurons, as well as skeletal muscle. Insulin secretion is controlled through a K_{ATP}-dependent mechanism when glucose levels increase, such as during a post-prandial state. In isolated pancreatic islets of wild type mice, 16.7 mM glucose resulted in a 6-fold higher rate of insulin secretion compared to

that at 2.8 mM glucose, while in mice lacking functional K_{ATP} channel activity (Kir6.2$^{-/-}$), glucose at 16.7 mM failed to cause any increase in insulin secretion above basal rates (Miki et al., 1998). Normally, the increase in intracellular glucose results in increased ATP, closing the channel. The resulting depolarization of the cell associated with decreased K^+ conductance leads to the activation of Ca_V channels allowing Ca^{2+} influx. The subsequent increase in $[Ca^{2+}]_i$ then activates the exocytosis of insulin-containing granules (Matin et al., 1989; Miki et al., 2005)

Glucagon secretion is also reliant upon a K_{ATP}-dependent mechanism. However, it does not appear to be at the level of the pancreatic α-cell, but rather through autonomic input to the pancreas (Miki et al., 2001). One example of this comes from the fact that there are no differences in glucagon secretion from isolated α-cells under hypoglycemic conditions between wild type and Kir6.2$^{-/-}$ mice. A second piece of evidence is that systemic hypoglycemia resulted in three-fold increase in glucagon secretion in wild type mice, while Kir6.2$^{-/-}$ mice exhibited defective glucagon secretion. Glucose-sensitive neurons were then found in the ventromedial hypothalamus (VMH) of wild type mice, which increased their firing rate when glucose levels increased. This was not observed in excised VMH neurons of wild type mice, yet it was observed in Kir6.2$^{-/-}$ mice. This suggests that glucose sensing is K_{ATP} channel-dependent. Finally, exposing these neurons to 2-DG to mimic a hypoglycemic condition resulted in glucagon secretion in wild type but not in Kir6.2$^{-/-}$ mice. Thus, K_{ATP} channels are required for glucagon secretion and do so through a central nervous system-mediated mechanism.

K_{ATP} channels are also directly involved in glucose uptake in skeletal muscle (Miki et al., 2002). Both basal and insulin-stimulated glucose uptake are elevated in muscles of Kir6.2$^{-/-}$ mice compared to wild type mice and to a greater extent in oxidative

rather than glycolytic muscles. A study employing double knockout mice (Kir6.2$^{-/-}$/IRS-1$^{-/-}$) provided evidence that K_{ATP} channel-mediated glucose uptake in these muscles is independent of the PI3 kinase signaling pathway (Minami et al., 2003).

Cytoprotection

A major function of K_{ATP} channels in muscles and neurons is thought to be protection against cellular damage during metabolic stress. In mice lacking functional K_{ATP} channels, significant damage was seen in skeletal muscle after four to five weeks of treadmill running (Thabet et al., 2005) or 28 days of swim training (Kane et. al, 2004). The latter study also reported significant cardiomyocyte damage as a result of intracellular Ca^{2+} overload. Thus, K_{ATP} channels are crucial in preventing fiber damage in cardiac and skeletal muscles during exercise and fatigue.

Two mechanisms so far have been identified to prevent fiber damage. The first one is maintenance of the resting membrane potential. During fatigue in skeletal muscle (Cifelli et al., 2008) and metabolic inhibition in both cardiac (Light et al., 1999) and skeletal muscle (Gramolini and Renaud, 1997), the resting membrane potential depolarizes by about 10-15 mV, i.e. from ~-80 mV to -65 or -70 mV. However, in the absence of K_{ATP} channel activity, the depolarization becomes excessive and the membrane potential reaches -30 mV, a potential known to activate L-type Ca^{2+} channels, or Ca_V. Opening of these channels allow for large Ca^{2+} influx and increased $[Ca^{2+}]_i$. As a consequence of the increased $[Ca^{2+}]_i$, proteases are activated, causing damage to the cell (Belcastro, 1993). Furthermore, the increased Ca^{2+} activates Ca^{2+}-ATPase and the sarcomere and thus myosin-ATPase, causing a further accentuated ATP utilization and stress.

The second mechanism is on the action potential. In cardiac muscle, Ca^{2+} entering

the cell during the plateau phase is shortened (Suzuki et al., 2002), while in skeletal muscle action potential amplitude is decreased (Gong et al., 2003). Consequently in both cases, less Ca^{2+} is released into the cell, decreasing the energy demand on Ca^{2+}- ATPase as well decreasing force production and thus the energy demand on myosin-ATPase. Overall, the role of the K_{ATP} channel is to preserve ATP during metabolic stress.

There have been few studies regarding the effect of K_{ATP} channels on energy metabolism. In one of these studies (Gramolini and Renaud, 1997), 60 min of metabolic inhibition caused a faster rate of ATP depletion in muscles with K_{ATP} channels blocked by glibenclamide compared to control muscles. However, the final extent was the same at the end of 60 min. In another study (Li, 2007), three min of fatigue caused greater ATP depletion during the first 120 sec of fatigue in Kir6.2$^{-/-}$ muscles compared to wild type muscles (Fig 1-1).

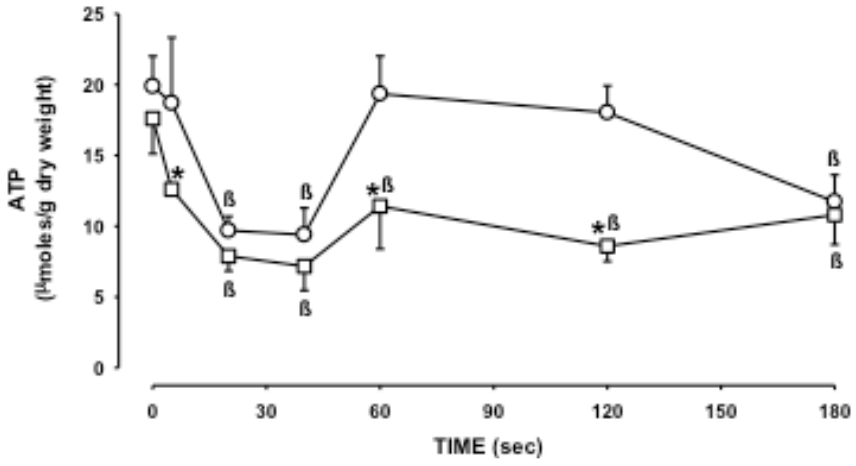

Figure 1-1. Kir6.2$^{-/-}$ FDB have significantly lower ATP levels during fatigue compared to wild type FDB. Fatigue was elicited with one contraction every sec for 3 min. Symbols: ○, wild type FDB; , Kir6.2$^{-/-}$ FDB. From Li, 2007.

Neither of these studies, however, suggest ATP levels become damaging when lacking K_{ATP} channel activity. In the study by Li (2007), although ATP levels are significantly lower during fatigue in Kir6.2$^{-/-}$ muscle, lactate production was less than that of wild type. This is surprising, as lactate would be expected to increase when ATP demand increases. Benkhalti (2007) did however show that during a 24 hour period, there is a greater oxygen uptake in Kir6.2$^{-/-}$ mice compared to wild type mice. Therefore, it is probable that more pyruvate enters the Krebs cycle in Kir6.2$^{-/-}$ mice. It is still not clear as to whether K_{ATP} channels prevent damaging ATP depletion or whether they prevent energy metabolism impairment, as initially proposed by Noma (1983).

The objective of this research project was to determine how the loss of K_{ATP} channel activity affects carbohydrate and energy metabolism during fatigue. The hypothesis was that "a lack of K_{ATP} channel activity impairs energy metabolism resulting in insufficient ATP production". To test this hypothesis, the following studies based upon specific aims were performed:

1) Determine the mobilization of glucose from glycogen and extracellular sources to calculate how many glucosyl units enters glycolysis.
2) Examine the fate of glucose by determining how much becomes lactate and how much is fully oxidized to CO_2.
3) Determine if there are increases in intermediates of metabolism and whether these are greater in Kir6.2$^{-/-}$ FDB.
4) Calculate the maximal ATP production from glucose metabolism and determine if it is higher in Kir6.2$^{-/-}$ FDB.

CHAPTER 2

MATERIALS AND METHODS

Animals and muscles

Experiments were carried out using 2- to 3-month-old wild-type C57BL6 and Kir6.2$^{-/-}$ mice (from Charles River, Canada). Kir6.2$^{-/-}$ mice are null mice for the gene that encodes for the Kir6.2 protein subunit that makes the pore of the K_{ATP} channel, and were generated as previously described (Miki et al. 1998). All mice weighed 20–25 g, were fed ad libitum, and housed according to the guidelines of the Canadian Council for Animal Care (CCAC). The Animal Care Committee of the University of Ottawa approved all experimental procedures used in this study. Mice were anaesthetized with a single intraperitoneal injection of 2.2 mg ketamine, 0.44 mg xylazine, and 0.22 mg acepromazine per 10 g of body mass. Following this, mice were sacrificed by cervical dislocation. Flexor digitorum brevis (FDB) muscles were excised from the hind paw and bundles controlling the 4th digit were separated from those controlling the 3rd digit by cutting away along the fascia that separates the two bundles, as described by Cifelli et al. (2008).

Physiological solution

FDB muscles were constantly immersed in physiological saline solution, even during the dissection. The control solution contained (in mM): 118.5 NaCl, 4.7 KCl, 2.4 $CaCl_2$, 3.1 $MgCl_2$, 25 $NaHCO_3$, 2 NaH_2PO_4, and 5.5 D-glucose. All solutions were continuously gassed with 95% O_2–5% CO_2 to keep pH at 7.4. Experimental temperature was 37°C for all experiments.

Force measurement

Muscles were attached with silk thread (Black Braided Silk Suture, 6-0, USA) to the stimulation apparatus. One end was attached to a stationary hook, while the other end was attached to a force transducer (Grass Instrument, Model FT03C, USA). The transducer was connected to a Grass Physiograph (Grass Instrument, Model 79E, USA). Maximum tetanic force was defined as the maximal force measured at the beginning of each experiment after the length had been adjusted. Thereafter, peak tetanic force was measured as the maximum force during a stimulation subsequent to the maximum force. Both maximum and peak tetanic force were calculated as the difference between the maximum force during a contraction and the baseline force measured 5 ms before a stimulation. Unstimulated force, defined as the amount of force exerted by a muscle without stimulation, was calculated as the difference in baseline just before a contraction was elicited and the baseline just before fatigue was elicited.

Stimulation and fatigue protocol

Electrical stimulations were applied across the two platinum wires (6 mm apart) located on opposite sides of the fibers. They were connected to a Grass S88 stimulator and a Grass SIU5 isolation unit (Grass Technologies/Astro-Med Inc.). Tetanic contractions were elicited with 200 msec trains of 0.3 msec, 12 V (supramaximal voltage) pulses at 200 Hz. Prior to fatigue, muscles were allowed to equilibrate for 30 min with one contraction every 100 sec. This ensured that the force generated by the muscle remained stable. For both wild type and Kir6.2$^{-/-}$ mice, muscles were discarded if the drop in peak tetanic force was greater than 10% as for previous experiments in this laboratory (Gong et al., 2000; Cifelli et al., 2007). Fatigue was elicited by reducing the interval of tetanic contraction from 100 sec to 1 sec. Muscles were allowed to recover from fatigue

while being stimulated every 100 sec.

Metabolite measurements

Muscles were frozen with clamps pre-cooled with liquid nitrogen (just prior to fatigue) at 60 and 180 sec or after 15 min of recovery. Muscles were stored at -80ºC until assays were performed. Muscles and physiological solutions were freeze-dried overnight using a lyophilizer (Freezemobile 6, Virtis, USA). Freeze-dried muscles were dissected free of any excess connective tissue, blood vessels and tendon and then weighed on an analytical balance (Mettler Toledo, XS105, USA).

Glycogen determination

Lyophilized muscle tissue was added to 1 N NaOH and incubated at 80ºC for 15 min to degrade endogenous glucose. The solution was neutralized by adding 66 µl each of 0.25 M HCl and 0.15 M sodium acetate buffer. Glycogen was hydrolyzed to glucose by adding 6 µl 1.5 g/L amyloglucosidase and incubating at 30ºC for 4 hours. Glucose content was determined enzymatically as described by Passoneau and Lowry (1983). Briefly, glucose was first coverted to glucose-6-phosphate (G-6-P) by hexokinase. G-6-P was converted to 6-phosphate-gluconolactone by G-6-P dehydrogenase, as follows:

$$\text{Glucose} + \text{ADP} \rightarrow \text{G-6-P} + \text{ADP}$$

$$\text{G-6-P} + \text{NADP}^{+} \rightarrow \text{6-phosphate-gluconolactone} + \text{NADPH} + \text{H}^{+}$$

Changes in NADPH fluorescence were measured using a fluorometer (Perkin Elmer, Model LS50B, USA). Glucose content was determined against a standard curve.

Glucose uptake

Glucose uptake was measured using 2-^{3}H-deoxyglucose (2-^{3}H-DG), a nonmetabolized glucose marker as described by Hansen et al. (1994), with a few

modifications. Briefly, 2.0 μCi/ml of 2-^{3}H-DG (Perkin Elmer, Woodbridge, ON) and 0.9 μCi/ml ^{14}C-sucrose (ARC chemicals, St. Louis, MO) were added 30 min prior to fatigue; i.e. at the start of the equilibrium period. Note that cold glucose was not replaced by 2-DG because this could alter metabolism. A previous study had shown that 2-^{3}H-DG uptake was not different whether cold 2-DG or cold glucose were used. [^{14}C]-sucrose was used to determine the extracellular volume so that the extracellular glucose could be subtracted from the total muscle glucose. After the experiment and subsequent freeze-drying, dry muscles were sonicated using a sonicator (Fisher Scientific, USA) in 0.5 ml of 6% perchloric acid (PCA). Homogenates were centrifuged for 15 min at 1,200 g. 2-[^{3}H]-DG and [^{14}C]-sucrose were counted from 480 μl of supernatant using a WinSpectral liquid scintillation counter (Model 1414, Perkin-Elmer Life Sciences, Boston, MA; Ecolume scintillation fluid, MPBIO, USA). Quenching was corrected by counting 100 μl of the 2-[^{3}H]-DG/[^{14}C]-sucrose physiological solution and 100 μl of the 2-[^{3}H]-DG/[^{14}C]-sucrose physiological solution in 480 μl of 6% PCA.

Lactate determination

Lyophilized muscles were exposed to 500 μl ice-cold 6% PCA and sonicated with a Microson ultrasonic cell disruptor (Heat System Ultrasonic Inc., USA) at maximum power for 15-20 sec. Homogenates were centrifuged for 30 min at 20,000 g (Beckman, Avanti J-25, USA) and supernatants were neutralized with ice cold 3 M K_2CO_3. K^+ salt was centrifuged (International Equipment Company, IEC, Micromax 3590F2282, USA) for 15 min at 10,000 g. Lactate content was determined enzymatically as described by Passoneau and Lowry (1983). Briefly, lactate was converted by lactate dehydrogenase to pyruvate, as follows:

$$\text{Lactate} + NAD^+ \leftrightarrow \text{Pyruvate} + NADH + H^+$$

Glutamate-Pyruvate Transaminase then maintained the reaction in favour of producing pyruvate, as follows:

$$\text{Pyruvate} + \text{Glutamate} \rightarrow \text{Alanine} + \alpha\text{-ketoglutarate}$$

Fluorescence of NADH was measured using a fluorometer, as described above and lactate content was determined using a standard curve.

Glucose oxidation

Following the equilibration period, muscles were exposed to cold physiological solution without any glucose or stimulation for 10 min. Following this washout period, muscles were exposed to physiological solution containing 2 μCi/ml D-[6-^{14}C]glucose for 10 min. Just prior to when fatigue was elicited, the bubbling of solution was stopped to prevent the loss of the $^{14}CO_2$. After freeze-clamping, muscles were quickly placed into rubber-capped vials and exposed to 1 ml of ice cold 1 M sulfuric acid, injected through the vial cap using a syringe. Liberated $^{14}CO_2$ was trapped inside the vial using 0.5 ml tubes containing 300 μl benzethonium hydroxide. Vials were then refrigerated to prevent any further metabolic reactions from occurring. Physiological solutions were also transferred to rubber-capped vials and injected with ice-cold PCA to give the final concentration of 6%. Vials were kept at room temperature and liberated $^{14}CO_2$ was captured as previously described. All 0.5 ml tubes containing trapped $^{14}CO_2$ were collected after 2 hours for reading by liquid scintillation (Cytoscint, MPBIO, USA,). Quenching was corrected by counting 100 μl of the D-[6-^{14}C]glucose physiological solution. Muscles were then freeze-dried and weighed as previously described.

Statistical analysis

Data are presented as means ± standard error (S.E.) with the number of samples

(n). Two way ANOVA was used to determine significant differences. ANOVA calculations were made using the version 9.2 GLM (General Linear Model) procedures of the Statistical Analysis Software (SAS Institute Inc., Cary, NC, USA). When a main effect or an interaction was significant, the least square difference (LSD) was used to locate the significant differences (Steel and Torrie, 1980). The word ‘significant' refers only to a statistical difference ($P < 0.05$).

CHAPTER 3

RESULTS

FORCE

Representive force traces of wild type and Kir6.2$^{-/-}$ FDB are shown in Appendix 1. Although the rate at which total force (which is represented by the peak of each contraction to the baseline of the first contraction) decreases similarly throughout the fatigue period, wild type and Kir6.2$^{-/-}$ FDB display differences in the type of force that is produced during the 180 sec fatigue period.

Peak tetanic force is the amount of force produced upon electrical stimulation. On average, the largest decreases in peak tetanic force occurred from the 10th to 60th sec for both wild type and Kir6.2$^{-/-}$ FDB (Fig 3-1A). The decreases in peak tetanic force for Kir6.2$^{-/-}$ FDB were significantly greater than for wild type FDB. For example, at 30 sec Kir6.2$^{-/-}$ had a 10% greater decrease in peak tetanic force. From the 60th to 180th sec, tetanic force did not change significantly for either wild type or Kir6.2$^{-/-}$ FDB, in that both remained at ~35% of pre-fatigue peak tetanic force. Unstimulated force occurrs when the muscle cannot fully relax between contractions. Unlike a tetanus, which last 200 ms, unstimulated force is constant. In wild type FDB, unstimulated force increased no more than 2% of the pre-fatigue peak tetanic force during the entire 180 sec fatigue bout (Fig 3-1C). By contrast, Kir6.2$^{-/-}$ displayed a sharp increase in unstimulated force to 29.5% by 30 sec. It then decreased to 22.4% at 60 sec, where it plateaued until the end of the fatigue bout. Force recovery after fatigue was greater in wild type FDB compared to Kir6.2$^{-/-}$

FIGURE 3-1

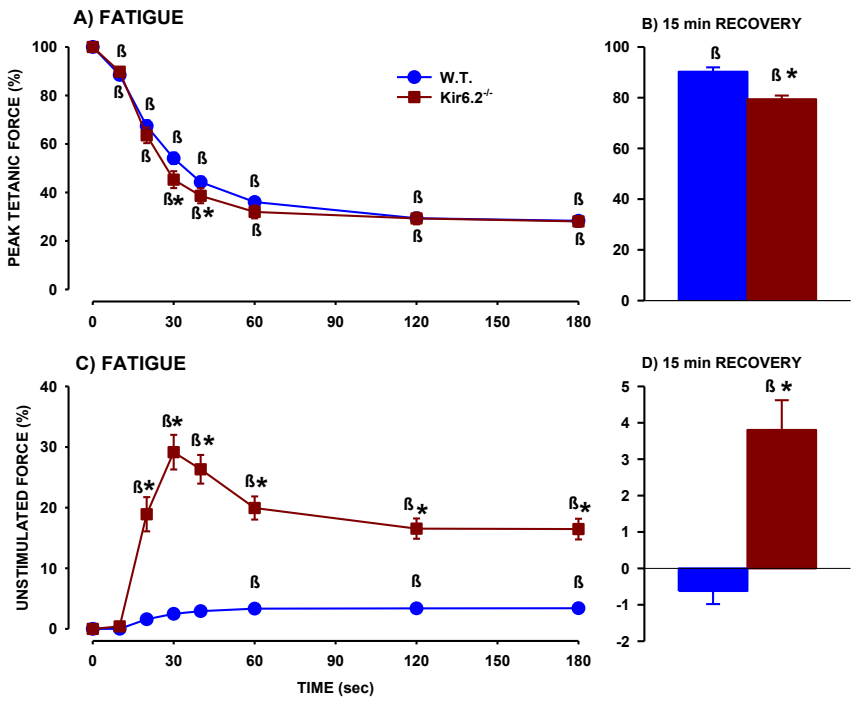

Figure 3-1. Peak tetanic force (A) decreased faster while the increase in unstimulated force (C) was much greater during the early phase of fatigue in Kir6.2$^{-/-}$ than in wild type FDB. FDB muscles were stimulated with one tetanic contraction per sec for 3 min and data are shown for every 10 sec. A) Peak tetanic force represents the force generated upon electrical stimulation. It was calculated as the difference between the peak of each contraction and the force 5 msec prior to contraction; it is presented as a percent of the pre-fatigue force. B) Peak tetanic force after 15 min of recovery. C) Unstimulated force occurrred when muscles failed to fully relax between contractions and is indicated by the increase in baseline force. It was calculated as the difference in baseline force 5 msec before a contraction and the baseline force prior to the first contraction; it is presented as a percent of the pre-fatigue peak tetanic force. D) Unstimulated force after 15 min of recovery.

* Significantly different from wild type FDB, § Significantly different from Time 0 sec, ANOVA, $P < 0.05$

FDB. Wild type FDB recovered 91% of peak tetanic force, while Kir6.2$^{-/-}$ FDB recovered only 79% (Fig 3-1B). By the end of the recovery phase, unstimulated force returned to pre-fatigue levels in wild type FDB (in fact baseline force decreased further than pre-fatigue levels by 0.5%) (Fig 3-1D). In contrast, Kir6.2$^{-/-}$ FDB still displayed 3.9% after 15 min of recovery.

All changes reported here during fatigue and recovery for peak tetanic force and unstimulated force are similar to those reported earlier by Cifelli et al. (2007). Furthermore, the authors had demonstrated that the faster decrease in peak tetanic force and lower force recovery is due to fiber damage and contractile dysfunction. In another study, Cifelli et al. (2008) demonstrated that the increase in unstimulated force is the result of excess Ca^{2+} influx through L-type Ca^{2+} channels.

GLUCOSE ENTRY INTO THE GLYCOLYTIC PATHWAY

There are two sources of glucose for glycolysis, one being glucose, stored in muscle as glycogen, and the other being extracellular glucose which is transported into the muscle cell at rest and during metabolic stress.

Glycogen breakdown

Wild type FDB had lower resting glycogen content compared to Kir6.2$^{-/-}$ FDB, the values being 112 and 131 μmoles/g dry weight, respectively (Fig 3-2). After the first 60 sec of fatigue, during which most of the decrease in peak tetanic force occurs, the decrease in glycogen content was 4 and 11 μmole/g dry weight for wild type and Kir6.2$^{-/-}$ FDB, representing a 2.6-fold difference. Interestingly, this period is also when unstimulated force dramatically increases in Kir6.2$^{-/-}$ FDB (Fig 3-1C). Glycogen content continued to decrease from the 60th to the 180th sec, reaching 69.3 μmoles/g dry weight in

FIGURE 3-2

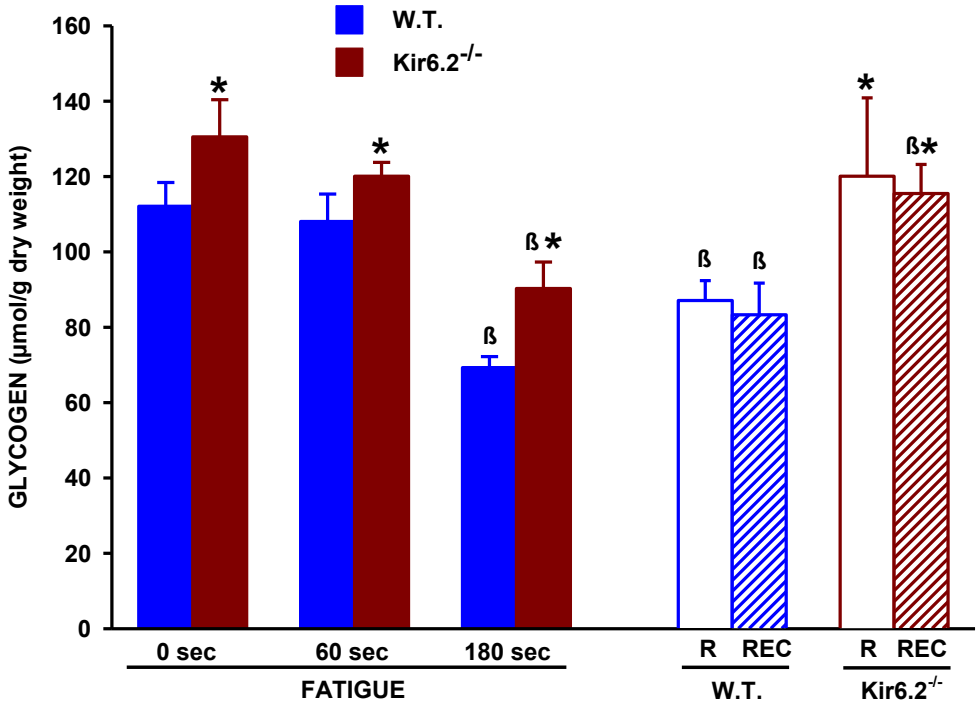

Figure 3-2. Glycogen content decreased to a greater extent in Kir6.2$^{-/-}$ FDB after 60 sec compared to wild type FDB, however at the end of 180 sec of fatigue there were no differences. Glycogen was measured in glucosyl units, which represent the number of glucose molecules for entry into glycolysis. REST (R) muscles were taken for comparison to fatigue. An additional set was taken to compare to recovery (REC) since glycogen levels decreased with the prolonged incubation. Vertical bars represent S.E. for 14-21 REST muscles and 4-7 FATIGUE/REC muscles.

* Significantly different from wild type FDB,

§ Significantly different from Time 0 sec,

ANOVA, $P < 0.05$

wild type and 90.3 μmoles/g dry weight in Kir6.2$^{-/-}$ FDB. Overall, wild type broke down 42.8 μmole glucosyl units/g dry weight compared to 40.2 μmole glucosyl units/g dry weight in Kir6.2$^{-/-}$ FDB. Following 15 min of recovery during which muscles were stimulated once every 100 sec, wild type FDB resynthesized less glycogen compared to Kir6.2$^{-/-}$ FDB. However, at that time glycogen levels were still 74% of pre-fatigue glycogen content in wild type FDB and 89% in Kir6.2$^{-/-}$ FDB. While these glycogen contents were lower than pre-fatigue levels, they were not different from the paired muscles that were unfatigued and sampled at the same time as the muscles fatigued and allowed to recover for 15 min.

Glucose uptake

Glucose uptake was measured using ^{3}H-2-deoxyglucose (^{3}H-2DG), a non-metabolized glucose analog, in the presence of 5.5 mM cold glucose. Cold glucose was not replaced by 2-DG in order to have normal energy metabolism during fatigue. Uptake of ^{3}H-2-DG is the same whether 2-DG or glucose is present in the physiological solution (Benkhalti, 2007). Resting values of glucose uptake were not significantly different between wild type and Kir6.2$^{-/-}$ FDB, being 11.6 and 11.2 μmoles/g dry weight, respectively (Fig 3-3). After 180 sec of fatigue, wild type FDB transported 18.0 μmoles/g dry weight compared to 20.6 μmoles/g dry weight for Kir6.2$^{-/-}$ FDB. This represented an increase of 6.41 and 9.34 μmoles/g dry weight above pre-fatigue levels. Glucose uptake was even greater after 15 min of recovery. Interestingly, the glucose uptake after 15 min recovery was not significantly greater than for those kept at rest the entire time, whereas for Kir6.2$^{-/-}$ FDB glucose uptake was 13.6 μmol/g dry weight greater in FDB that were fatigued and allowed to recover compared to those kept at rest.

FIGURE 3-3

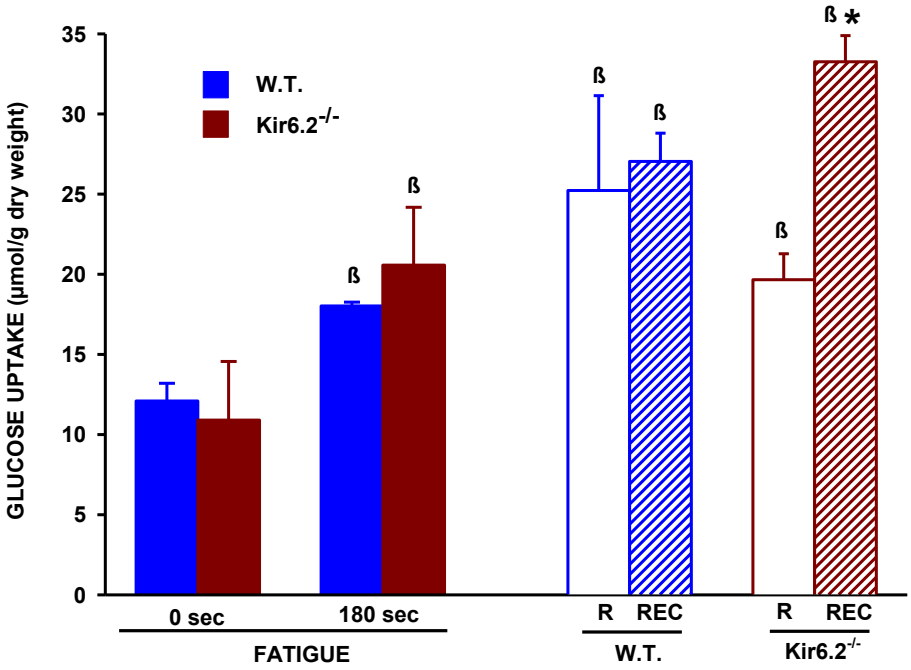

Figure 3-3. Kir6.2$^{-/-}$ FDB transported more glucose during fatigue and recovery, but resting levels were not different. Glucose uptake was measured using the non-metabolized glucose marker ^{3}H-2-deoxyglucose (2 µCi/ml) in the presence of 5.5 mM glucose. 0.9 µCi/ml ^{14}C-sucrose was added to determine the extracellular volume. Glucose uptake was calculated as the difference between the total cell volume and the extracellular volume multiplied by specific activity of ^{3}H-2-deoxyglucose. Vertical error bars represent the S.E. for 3 muscles.

* Significantly different from wild type FDB,

§ Significantly different from Time 0 sec,

ANOVA, $P < 0.05$

END PRODUCTS OF GLUCOSE METABOLISM

Glucosyl units are ultimately broken down by glycolysis to pyruvate. At that point there are two possible fates for pyruvate: 1) the cytosolic lactate dehydrogenase, which converts pyruvate to lactate; or 2) pyruvate dehydrogenase within the mitochondria, which decarboxylates pyruvate to acetyl-CoA and enters the Krebs cycle to eventually produce CO_2.

Lactate production during muscle preparation

In a previous study, unexpectedly high lactate levels had been found in the physiological solution that bathed the muscles (Li and Renaud, unpublished results). It was then suspected that a large portion of this lactate may have come from a large production during the muscle preparation. Experiments were therefore designed to determine the extent of that lactate production and how it can influence the measurements during the fatigue period.

In one experiment, muscles were tested in pairs for which one muscle was kept in the same physiological solution for the entire duration of the experiment while for the other muscles the physiological solution was changed three times, the last one being just before fatigue. This test revealed a three-fold difference in physiological solution lactate measurement when solutions were not changed prior to fatigue, that is, the physiological solution contained 150 μmoles/g dry weight compared to 48.1 μmoles/g dry weight when they were not changed (Fig 3-4). In a second experiment, lactate was measured in physiological solution after the muscle length had been adjusted to generate maximum force. Interestingly, the lactate

FIGURE 3-4

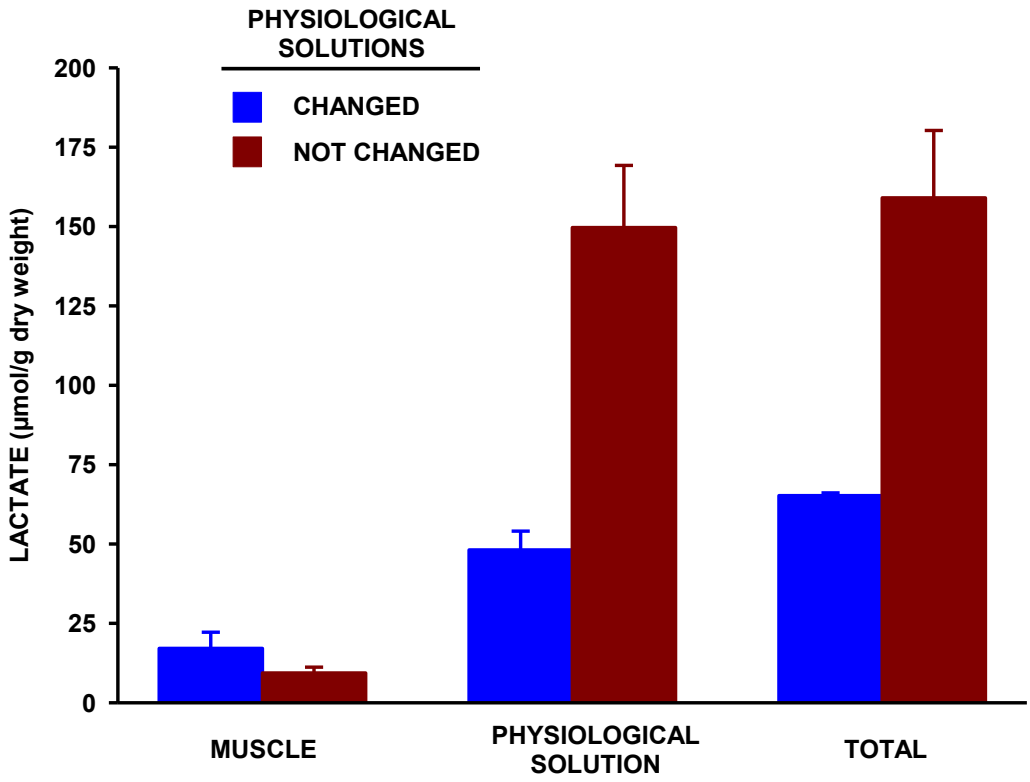

Figure 3-4. After 3 min of fatigue, there were large differences in lactate contents when solutions were or were not changed prior to fatigue. Paired muscles were used. For both muscles, length was adjusted for maximum force followed by 30 min equilibration before fatigue was elicited with one contraction per sec for 3 min. Muscles were freeze-clamped in liquid nitrogen at the end of fatigue and lactate was determined in both muscles and physiological solution. For one paired muscle the same physiological solution was kept for the entire experiment while for the other paired muscle, solutions were changed three times; i.e. after MAX, 15 min of EQUIL, 30 min of EQUIL (the latter being just before fatigue). Vertical bars represent S.E. for 5 muscles.

* Significantly different from wild type FDB,

§ Significantly different from Time 0 sec,

ANOVA, $P < 0.05$

content was 51 μmoles/g dry weight (Fig 3-5), a value similar to the content after fatigue when solution was changed just before fatigue (Fig 3-4). Physiological solution was then changed after 15 min of equilibrium. At that time one muscle was touched with a Kimwipe to remove all the physiological solution around the muscle (WIPE), while for the other paired muscle the fluid was not removed (NO WIPE). Lactate values of WIPE muscles were lower, being 15.1 μmoles/g dry weight compared to NO WIPE muscles, which had lactate content of 21.8 μmoles/g dry weight. When the same procedure was repeated after 30 min of equilibrium, the physiological solution from the WIPE muscle contained less lactate than the NO WIPE, albeit the difference was smaller than at 15 min.

To clearly see the importance of wiping muscles when solutions were changed, lactate from the physiological solution that incubates the muscle was measured at 20, 60 and 180 sec of fatigue (Fig 3-5). When the muscle was wiped just prior to fatigue, lactate increased as the duration of stimulation increased from 20 to 180 sec. These values were 2.6, 4.9 and 6.3 μmole/g dry weight, respectively. The lactate contents in the NO WIPE condition were considerably more variable during fatigue, with lactate levels of 9.8, 3.0 and 5.9 μmoles/g dry weight at 20, 60 and 180 sec, respectively. The largest difference is seen early in fatigue at 20 sec, where the lactate in physiological solution from muscles that were not wiped were 3.8 times greater than those that were wiped (Fig 3-5). Based upon these results, all remaining experiments were adjusted so that physiological solutions were always changed after MAX as well as at 15 min EQUIL, 30 min EQUIL (the latter being just before the fatigue bout). Also, a Kim wipe was applied to muscles before adding new solutions. Importantly, the methods carried out for these experiments were applied to other metabolite experiments as well, as they were carried

FIGURE 3-5

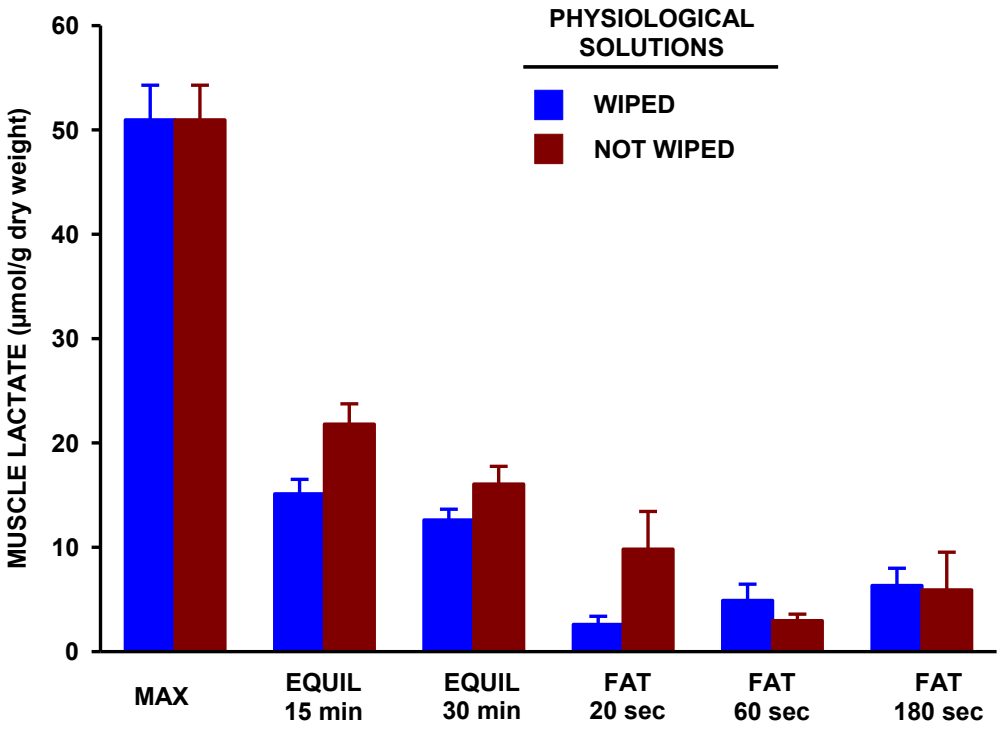

Figure 3-5. Wild type FDB muscles released large amounts of lactate into physiological solution following dissection leading to contamination when solutions are changed. Lactate was measured in physiological solution at the end of the maximization period (MAX). Solutions were then changed after 15 and 30 min of equilibrium (EQUIL), the latter being just before a fatigue bout of 20, 60 or 180 sec. Fatigue was elicited with one contraction per sec for the duration of fatigue. Experiments were carried out using paired muscles in which for one the application of a Kimwipe was used to remove excess fluid surrounding muscles between solution changes (WIPED). Vertical bars respresent the S.E. for 30 muscles (MAX), 15 muscles (EQUIL) and 5 muscles (FAT).

* Significantly different from wild type FDB,

§ Significantly different from Time 0 sec,

ANOVA, $P < 0.05$

out prior to performing all glycogen, glucose uptake, glucose oxidation experiments in addition to lactate experiments. Due to the incubation times needed with radioactive ligands, glucose uptake and oxidation experiments were not able to have solutions changed and muscles wiped just prior to fatigue, yet all other changes prior to fatigue were carried out to remain as consistent as possible.

Lactate production during fatigue

Prior to fatigue, wild type FDB muscles had slightly lower resting muscle lactate than Kir6.2$^{-/-}$ FDB with levels being 10.4 and 14.3 μmole/g dry weight, respectively (Fig 3-6A). At 60 sec of fatigue, lactate levels in wild type muscle had increased to 33.9 μmole/g dry weight, whereas in Kir6.2$^{-/-}$ muscle, levels had increased to only 27.7 μmoles/g dry weight. This represented values of 23.5 and 13.4 μmoles/g dry weight above resting levels during the first 60 sec. At the end of the the 3 min fatigue bout, muscle lactate was 21.9 μmole/g dry weight in wild type FDB and 22.0 in Kir6.2$^{-/-}$ FDB. After 15 min of recovery, muscle lactate was higher in wild type muscle (4.9 μmole/g dry weight) than in FDB lacking K_{ATP} activity (3.2 μmole/g dry weight). These lactate contents were not significantly different from those of paired muscles that were not fatigued but sampled at the same time as for the recovery period. Except for resting levels, most of the lactate produced was found in the physiological solution. Resting levels of lactate in the incubating solution (extracellular lactate) of wild type FDB were 7.5 μmole/g dry weight, compared to 10.2 μmole/g dry weight for Kir6.2$^{-/-}$ FDB (Fig 3-6B). For wild type FDB, extracellular lactate increased throughout the fatigue period and during recovery, reaching 43.6 μmoles/g dry weight after 180 sec and 133.1 μmoles/g dry weight after the recovery. For Kir6.2$^{-/-}$ FDB, lactate

FIGURE 3-6

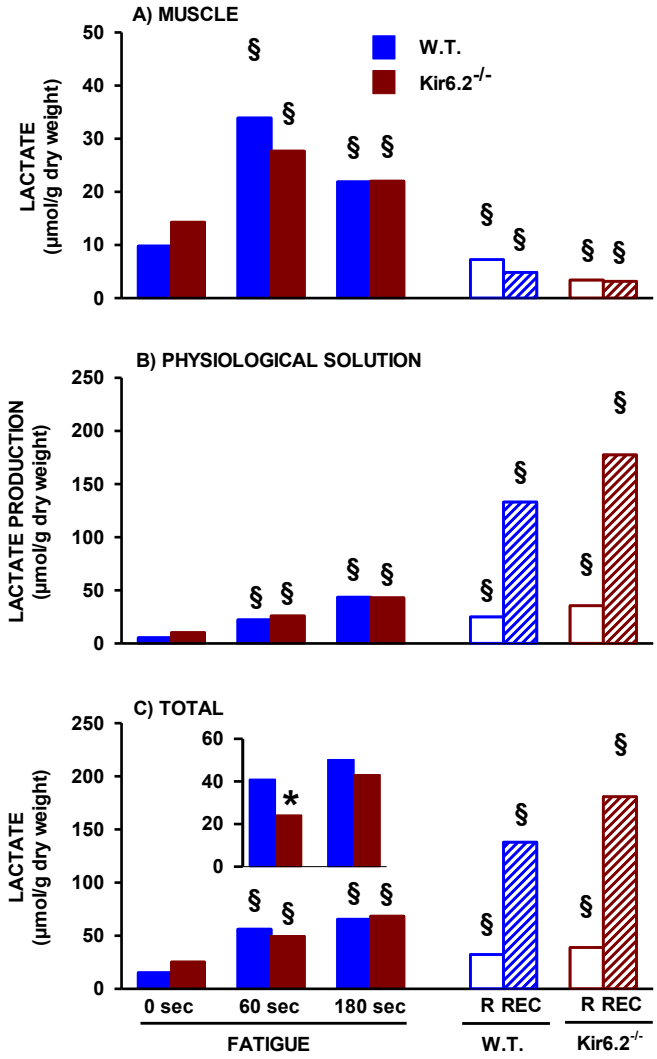

Figure 3-6. Lactate production was significantly less in Kir6.2$^{-/-}$ than in wild type FDB only during the first 60 sec of fatigue. Inset in (C) shows the increases in total lactate contents at 60 and 180 sec calculated as a difference in mean values at 0 sec. Fatigue was elicited with one contraction per sec for duration of fatigue. During recovery from fatigue, muscles were stimulated once every 100 sec. Vertical bars represent S.E. for 20 muscles (0 sec) and 5 muscles (FATIGUE, muscles not stimulated paired to recovered muscles [R], and recovery [REC]).

* Significantly different from wild type FDB,

§ Significantly different from Time 0 sec,

ANOVA, $P < 0.05$

during the fatigue period increased similarly with no differences compared to wild type FDB, however there was a greater amount after the recovery period, reaching 180.7 μmoles/g dry weight, a level 33% greater than seen in wild type FDB.

Adding all muscle and extracellular lactate values, the largest increase during fatigue for both wild type and Kir6.2$^{-/-}$ FDB was during the first 60 sec (Fig 3-6C). Interestingly, despite the large development of unstimulated force during that time, the net increase, calculated as the difference between zero and 60 sec was two-fold greater in wild type FDB as opposed to Kir6.2$^{-/-}$ FDB (Fig 3-6C, inset). However, after 180 sec of fatigue this difference is no longer present as net lactate production in wild type FDB was 47.6 μmoles/g dry weight compared to 43.2 μmoles/g dry weight in Kir6.2$^{-/-}$ FDB. Compared to muscles kept at rest, muscles recovering from fatigue produced significant lactate, being greater in Kir6.2$^{-/-}$ FDB than wild type FDB (Fig 3-6C).

CO_2 production

Test for altered metabolism if solution was not gassed during fatigue bout

The extent of glucose oxidation was measured by determining the amount of $^{14}CO_2$ produced from 2 μCi/ml of D-[6-^{14}C] glucose added prior to fatigue. In the previous experiments the apparatus allowed for the continuous bubbling of the physiological solution with 95% O_2: 5% CO_2 to maintain proper oxygen levels and pH. However, such bubbling may saturate the benzethonium hydroxide used to catch CO_2 or create a loss of $^{14}CO_2$ in the air. So it was important that during incubation in the presence of ^{14}C-glucose that the bubbling was stopped. The bubbling was also important as a means to keep fluid moving around the muscle and stopping it may also affect O_2 availability to muscles. If a hypoxic core developed to a greater extent when the bubbling

FIGURE 3-7

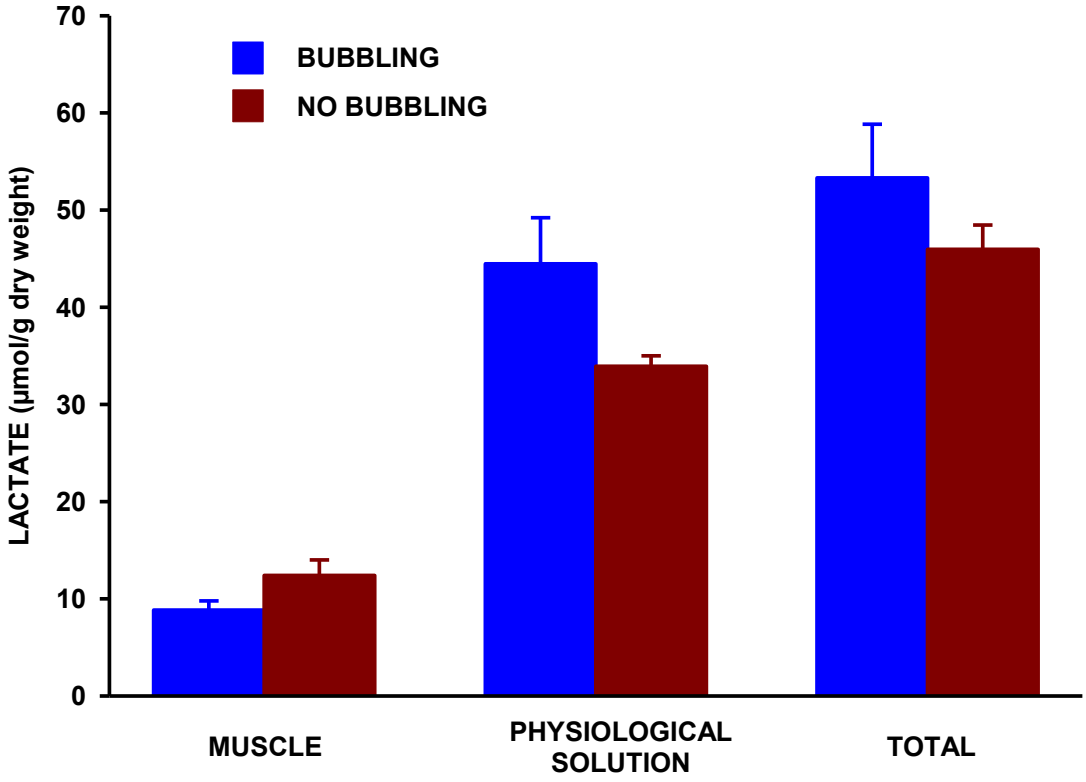

Figure 3-7. There is no significant difference in lactate production if continuous oxygenation is present during a 3 min fatigue bout. Paired muscles were used. For both muscles, length was adjusted for maximum force followed by a 30 min equilibration before fatigue was elicited with one contraction per sec for 3 min. Muscles were freeze-clamped in liquid nitrogen at the end of fatigue and lactate was determined in both muscles and physiological solution. Fatigue was elicited with one contraction per sec for duration of fatigue. Vertical bars represent S.E. for 5 muscles.

* Significantly different from wild type FDB,

§ Significantly different from Time 0 sec,

ANOVA, $P < 0.05$

stopped, then more lactate would be produced (Barclay et al., 2005). Lactate levels after 3 min of fatigue were therefore determined for which one of the paired FDB was fatigued while bubbling was not interrupted and for the other paired FDB for which bubbling was interrupted when fatigue was induced.

The lactate levels produced during fatigue with and without bubbling were not significantly different, being 53.3 and 46.0 μmoles/g dry weight, respectively (Fig 3-7). More importantly, the lactate level was not greater when the solution was not bubbled. Therefore bubbling was stopped during the fatigue period for the measurement of $^{14}CO_2$.

Glucose oxidation ($^{14}CO_2$) production during fatigue

Most of the $^{14}CO_2$ generated during fatigue was found in the physiological solution with very little $^{14}CO_2$ in the muscle (Fig 3-8A,B). Resting total $^{14}CO_2$ was slightly lower in wild type FDB, being 2.16 μmoles/g dry weight compared to 2.44 μmoles/g dry weight in Kir6.2$^{-/-}$ FDB (Fig 3-8C). From 0 to 60 sec, $^{14}CO_2$ production increased only minimally (0.4 μmoles/g dry weight) in wild type, while for Kir6.2$^{-/-}$ FDB levels almost doubled. From 60 to 180 sec $^{14}CO_2$ production did not increase for wild type and did not further increase for Kir6.2$^{-/-}$ FDB. Overall during fatigue, wild type FDB produced only 0.7 μmoles/g dry weight $^{14}CO_2$ above rest. Kir6.2$^{-/-}$ however, generated twice as much $^{14}CO_2$ compared to wild type FDB during fatigue. For both wild type and Kir6.2$^{-/-}$ FDB, there was an increase in $^{14}CO_2$ production during recovery from fatigue. Wild type FDB produced 1.78 μmoles/g dry weight during recovery while Kir6.2$^{-/-}$ FDB produced a greater amount, being 3.0 μmoles/g dry weight. Overall, Kir6.2$^{-/-}$ FDB oxidized a greater amount of glucose compared to wild type FDB during both fatigue and recovery, measured through $^{14}CO_2$ production.

FIGURE 3-8

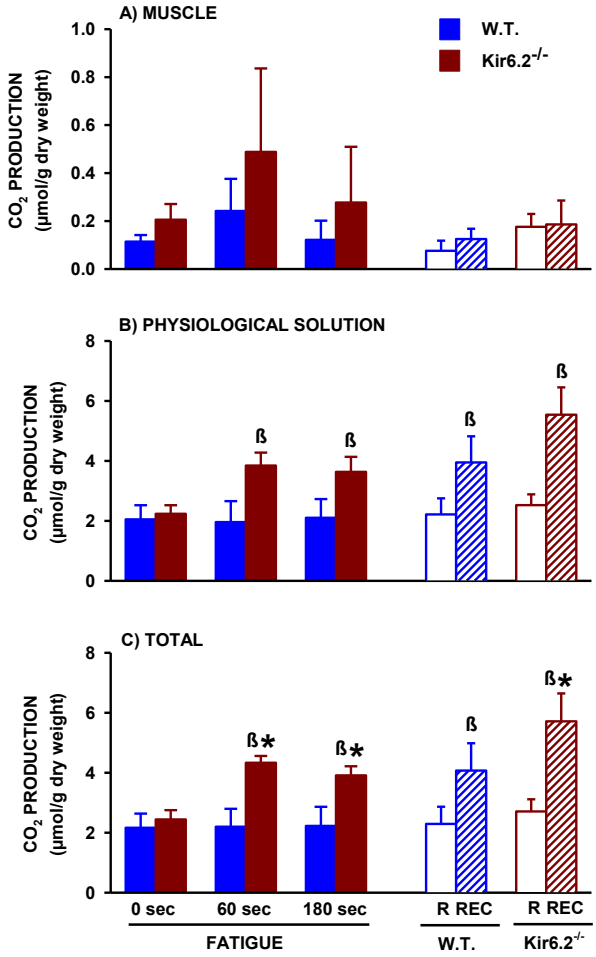

Figure 3-8. Compared to wild type FDB, Kir6.2$^{-/-}$ FDB oxidized more glucose to CO_2 during fatigue as well as during recovery from fatigue. After maximization and equilibrium, glucose oxidation was measured by adding ^{14}C-6-glucose to the physiological solution incubating the muscle. Fatigue was elicited by one contraction every sec. During recovery from fatigue, muscles were stimulated once every 100 sec. After the experiment was finished, the resulting $^{14}CO_2$ was released from either the muscle or physiological solution by the addition of 1 M sulfuric acid and 6% perchloric acid.

* Significantly different from wild type FDB,

§ Significantly different from Time 0 sec,

ANOVA, $P < 0.05$

CHAPTER 4

DISCUSSION

It is now proposed that fatigue is a protective mechanism preventing damage to muscle fibers from excessive energy depletion or large increases in $[Ca^{2+}]_i$ (McKenna et al., 2008). The K_{ATP} channel is believed to play a crucial role in myoprotection during exercise, since lacking channel activity results in contractile dysfunction, excess $[Ca^{2+}]_i$ and fiber damage (Light et al., 1994; Kane et al., 2004; Thabet et al., 2005; Cifelli et al., 2007). Compared to wild type, Kir6.2$^{-/-}$ FDB break down ATP to a greater extent during the first 120 sec of fatigue (Fig 1-1). However, there is little knowledge about how the K_{ATP} channel affects energy metabolism. Therefore, the objective of this study was to examine how K_{ATP} channels affect energy metabolism during muscular activity leading to fatigue. Glucose metabolism was investigated while fatigue was elicited in flexor digitorum brevis muscles lacking K_{ATP} channel activity.

The major findings of this study were that: 1) the initial decrease, but not the final extent, in glycogen is greater in Kir6.2$^{-/-}$ FDB compared to wild type FDB; 2) glucose uptake in Kir6.2$^{-/-}$ FDB is greater after fatigue and especially after 15 min of recovery compared to wild type FDB; 3) lactate production is less during fatigue but greater during recovery in Kir6.2$^{-/-}$ FDB compared to wild type; and 4) Kir6.2$^{-/-}$ FDB oxidize more glucose compared to wild type during fatigue and recovery.

ENERGY METABOLISM DURING FATIGUE

CHANGES IN GLYCOGEN

On average, resting glycogen stores in wild type FDB were 112 μmoles/g dry weight, similar to those seen in other studies involving isolated muscles which range

between 113 to 146 μmoles glucosyl units/g dry weight (Spriet et al., 1989; Spriet et al., 1990, Lai et al., 2009). The 38% decrease in resting glycogen during fatigue in the current study is also comparable, albeit slightly greater, to other studies where the average decreases in glycogen were 19 – 27% from rest after 3 min of stimulation at one contraction per sec. However, the isolated muscles in these studies may have relied more on extracellular glucose since they used 8 mM glucose compared to 5.5 mM in this study (Derave et al., 2000; Ihlemann et al., 2000; Ihlemann et al., 2001). Glycogen decreases up to 50% during 60 sec of fatigue is only observed when the circulation to the muscle is prevented, so the muscle has greater reliance upon glycolysis from glycogen stores (Spriet et al., 1989; Spriet et al., 1990).

Compared to wild type FDB, Kir6.2$^{-/-}$ FDB had, at rest, 29% higher glycogen content. This may be explained by an increase in basal glucose uptake in Kir6.2$^{-/-}$ mice in vivo. Miki and colleagues (2002) demonstrated that in vivo Kir6.2$^{-/-}$ EDL muscles, as well as white and red gastrocnemius muscles, have greater basal glucose uptake. Glucose uptake was not measured in FDB muscles in the study, however EDL and FDB share similar glycolytic fiber type similarities, as the percentage of fibers expressing fast-glycolytic MHC IIX are 72 and 56% in FDB and EDL, respectively. FDB muscles also have 67% of fibers expressing MHC IIA, similar to slow-twitch soleus muscles, which have 40% of fibers that express MHC IIA (Banas et al., 2011). All Kir6.2$^{-/-}$ muscles were shown to have a greater sensitivity to 100 μU insulin/mL than wild type, especially in oxidative muscles such as soleus. Therefore, in vivo Kir6.2$^{-/-}$ FDB muscles are transporting more glucose at rest, which can then result in higher hexokinase-mediated glucose phosphorylation to glucose-6-phosphate (a substrate for glycogen synthase), thus increasing glycogen storage compared to wild type mice.

Compared to wild type, Kir6.2$^{-/-}$ FDB broke down approximately twice as much glycogen during the first 60 sec of stimulation with levels decreasing by 10.4 μmoles/g dry weight compared to 4.0 in wild type. The fact that Kir6.2$^{-/-}$ FDB had higher resting levels of glycogen than wild type is unlikely to be the reason as to why the extent of glycogen breakdown was higher. Studies have indicated that there is no difference in glycogenolysis, PHOS *a* activation or extent of glycogen breakdown with varying resting glycogen contents (Ren and Hultman, 1990; Spriet et al., 1990; Spencer and Katz; 1991). Instead the greater glycogen breakdown may be explained through two reasons: 1) $[Ca^{2+}]_i$, and 2) an increased energy demand leading to increases in AMP and P_i levels as well as the activation of AMPK.

Wild type FDB developed negligible unstimulated force during the first 60 sec. However, in Kir6.2$^{-/-}$ FDB unstimulated force was almost 30% of pre-fatigue peak tetanic force. Unstimulated force is due to increased $[Ca^{2+}]_i$ (Cifelli et al., 2007; Cifelli et al., 2008; Boudreault et al., 2010). At rest, $[Ca^{2+}]_i$ is approximately 30 nM, increasing during fatigue to 100 nM in wild type FDB. However, the increase can be much higher in Kir6.2$^{-/-}$ FDB, being 250 nM. Glycogenolysis is regulated by the enzyme glycogen phosphorylase (PHOS) which catalyzes the hydrolysis of glycogen into glucose-1-phosphate at the alpha-1,4-glycosidic bond. PHOS has two forms: the less active, unphosphorylated *b* form and the active, phosphorylated *a* form. Ca^{2+} upregulates PHOS kinase, which converts PHOS *b* to PHOS *a* (Fischer and Krebs, 1955; Drummond et al., 1969; Brostrom et al., 1971). It is therefore more than likely that the higher $[Ca^{2+}]_i$ in Kir6.2$^{-/-}$ FDB fibers increases the activity of PHOS kinase and subsequently PHOS *a* to greater extent in these muscles.

Unstimulated force in Kir6.2$^{-/-}$ FDB is constant, as opposed to a 200 msec tetanic

contraction; i.e. myosin-ATPase is constantly consuming ATP. The same is true for the Ca^{2+}-ATPase pump as it tries to transport Ca^{2+} back into the SR. Together, these two events impose a much higher energy demand, increasing ATP utilization. Considering the large ATP depletion in Kir6.2$^{-/-}$ FDB from 18 μmoles/g dry weight at rest to 8 μmoles/g dry weight during fatigue (Fig 1-1), it is then very likely that the subsequent increase in ADP leads to: i) increased P_i; and ii) increased AMP via the adenylate kinase reaction (Krause et al., 1996; Gorostioga et al., 2010). AMP increases activity of PHOS *a* allosterically (Lowry et al., 1964). In fact, there was a dose-dependent response in skeletal muscle PHOS *a* activity by the addition of AMP, whereby at 0.1 μM AMP activity of PHOS *a* was 292 U/mg and increased to 497 U/mg with the addition of 100 μM AMP (Rush and Spriet, 2001). P_i is another activator of PHOS and its effect is AMP-dependent: the K_m for P_i decreases from 27 mM to 6 mM when [AMP] was increased from 0.1 mM to 2 mM (Ren et al., 1990).

Finally, the decrease in ATP and subsequent increase in AMP is more than likely to activate AMPK, which is known to be activated during exercise and especially during a metabolic stress leading to a decrease in ATP (Park et al., 2002; Birk et al., 2006). Glycogen phosphorylase activity increases ~50% when AMPK is activated by 4 mM AICAR (Young et al., 1996). Furthermore, Ca^{2+} is known to quickly activate AMPK through a Ca^{2+}-dependent calmodulin protein kinase-β mechanism, irregardless of levels of AMP (Hawley et al., 2005; Woods et al., 2005). Therefore, the greater glycogen breakdown in Kir6.2$^{-/-}$ FDB during the first 60 sec of fatigue is most likely due to higher [Ca^{2+}]i and the activation of glycogenolytic enzymes from increased ATP breakdown products.

Interestingly, from the 60th to the 180th sec of fatigue, the differences in glycogen

depletion between wild type and Kir6.2$^{-/-}$ FDB became much smaller, being 27.3 and 29.8 μmoles/g dry weight, respectively. These results were unexpected because of the still larger unstimulated force and Ca^{2+} in Kir6.2$^{-/-}$ FDB. It is also important to note that during that time ATP levels did not increase back towards pre-fatigue levels as occurred in wild type FDB (Fig 1-1). Thus, more glycogen should have been used in Kir6.2$^{-/-}$ FDB.

Acidic pH decreases PHOS activity through a negative feedback mechanism during exercise. For example, cycling exercise causing a decrease in pH to 6.82 compared to a cycling exercise decreasing pH to 7.02 decreases the fraction of active PHOS α by almost one-third. One would expect that the higher metabolic demand from unstimulated Ca^{2+} and force would then result in lower pH. However the amount of lactate produced at the end of the fatigue period was similar between wild type and Kir6.2$^{-/-}$ FDB. Therefore, lower intracellular pH (pH_i) from lactic acid in Kir6.2$^{-/-}$ is unlikely unless the greater net hydrolysis in ATP observed in Kir6.2$^{-/-}$ contributes to a lower pH_i, but this remains to be determined. A more likely explanation is that although there is a greater energy demand in Kir6.2$^{-/-}$ FDB during this time in fatigue, a metabolic impairment prevents the proper mobilization of glycogen. This may in fact be responsible for the previous observation that Kir6.2$^{-/-}$ FDB do not maintain proper ATP levels as wild type FDB do (see section entitiled "CARBOHYDRATE METABOLISM AND ENERGY BALANCE" for further discussion on this issue).

GLUCOSE UPTAKE DURING FATIGUE

Previous studies reported glucose uptake ranging from 25 – 30 μmole/hour/g wet weight during 10 – 20 min of stimulation, which would convert, on average, to ~ 5 μmole/g dry weight over 3 min (Ihlemann et al., 2000; Abbott et al., 2011). The rate of glucose uptake reported in this study for wild type FDB was similar, being 6.41 μmoles/g

dry weight. The contraction-mediated glucose uptake measured after 180 sec of fatigue gave rise to a 1.5-fold greater uptake in Kir6.2$^{-/-}$ FDB than in wild type FDB. Here, it is suggested that the factor causing differences in glycogen breakdown between the two muscles played a similar role for the glucose uptake. During contraction, GLUT4s are transported to the cell membrane to increase their number in order to transport more glucose into the active muscle cell (Niu et al., 2010). This process involves the exocytosis of intracellular GLUT4 vesicles for which Ca^{2+} plays a large role. Inhibiting Ca^{2+} reuptake into the SR following contraction increases glucose transport in muscle (Sorensen et al., 1980; Clausen et al., 1981). Caffeine exposure to stimulate greater Ca^{2+} release resulted in a three-fold increase in glucose uptake, while the addition of dantrolene, a SR Ca^{2+}-release blocker, markedly decreased glucose transport to nearly resting levels (Wright et al., 2004). Thus, it is more than likely that the higher $[Ca^{2+}]$i in Kir6.2$^{-/-}$ results in greater glucose uptake.

As with glycogen, AMPK may also be a major factor in explaining the differences in glucose uptake between wild type and Kir6.2$^{-/-}$ FDB. The activation of AMPK during contraction causes the translocation of GLUT4 to the sarcolemma and, consequently, increases glucose transport (Nakano et al., 2006). When gastrocnemius muscles are stimulated every sec for five min, AMPK activity is increased 100% even when the increase in AMP was very modest (~0.4 nmol/g wet weight) (Park et al., 2002). Interestingly, AMPK can also be indirectly activated through Ca^{2+} via calcium/ calmodulin-dependent kinase kinase (CaMKK) (Abbott et al., 2009). Considering the decreased ATP content and increased $[Ca^{2+}]_i$ in Kir6.2$^{-/-}$ FDB compared to wild type FDB (Li, 2007), a role of AMPK in the increase in GLUT4 content cannot be ignored after 3 min of fatigue, as well as on recovery from fatigue.

END PRODUCTS OF GLUCOSE METABOLISM

As expected, muscle lactate increased with the number of contractions reaching 33.9 μmoles/g dry weight after 180 sec of fatigue in wild type FDB. The results from this study are on the lower end of values ranging from 32 to 104 μmoles/g dry weight reported by others (Côté et al., 1997; Dawson et al., 2005; Gibala et al., 2009). For this study, the main differences in total lactate production between wild type and Kir6.2$^{-/-}$ FDB during fatigue occurred at 60 sec (Fig 3-6C). The increases in lactate above resting levels were 38.3 μmoles/g dry weight in wild type compared to only 24.2 μmoles/g dry weight in Kir6.2$^{-/-}$ FDB, a 37% difference. While this is in agreement with the results from Li (2007), where lactate was also greater in wild type compared to Kir6.2$^{-/-}$ during fatigue, it is surprising that lactate production was significantly less in Kir6.2$^{-/-}$ FDB considering the greater ATP demand and the much lower ATP compared to wild type FDB.

In contrast to an increase in lactate production, there is a greater oxidation of glucose in Kir6.2$^{-/-}$ FDB. In wild type FDB, at 60 sec, the production of $^{14}CO_2$ is very minimal being only 0.04 μmoles/g dry weight higher than resting levels. This was expected, as the reliance upon glucose oxidation does not normally become predominant at such an earlier period of contraction. PCr, on the other hand, is heavily relied upon up to 50 sec of contraction/exercise. Indeed, the decrease in PCr from Li (2007) suggests during the first 30 sec of fatigue PCr degradation is a main source of energy, while further contraction to 60 sec is reliant upon glycolysis. It appears that when muscle lacks K_{ATP} channel activity during fatigue, the reliance upon glucose oxidation becomes much greater during the first 60 sec of fatigue, perhaps due to faster activation of mitochondrial activity. It is also consistent with the results from Benkhalti (2009), which demonstrate

that Kir6.2$^{-/-}$ mice have a higher VO_2 compared to wild type.

Ca^{2+} may also play a role in the increased oxidation of glucose at the level of pyruvate dehydrogenase. Ashour and Hansford (1983) demonstrated that PDH increased from the inactivated state to activated state with increasing Ca^{2+} concentration. Since the increase in unstimulated force/Ca^{2+} is the greatest at 30 sec of fatigue in Kir6.2$^{-/-}$, reaching ~30% of initial maximal force, compared to a negligible rise in wild type FDB, this constant presence of Ca^{2+} in Kir6.2$^{-/-}$ may activate PDH to a much greater extent, allowing for a greater amount of pyruvate into the mitochondria to be converted to acetyl-CoA, eventually becoming oxidized to CO_2.

It is interesting that from 60 to 180 sec, Kir6.2$^{-/-}$ fail to increase the oxidation of glucose any further (Fig 3-8C). This is at a point when the amount of tetanic force generated is at its lowest, lowering the energy demand upon myosin-ATPase. However, the unstimulated force remains high, thus constantly requiring ATP for myosin crossbridge cycling. It would be expected that oxidation of glucose would keep increasing in Kir6.2$^{-/-}$ FDB.

GLUCOSE METABOLISM DURING RECOVERY

After fatigue when muscles were allowed to recover at one contraction per sec for 15 min, glycogen recovered to a greater extent in Kir6.2$^{-/-}$ FDB, possibly due to a greater amount of glucose entering the cell to become stored as glycogen by glycogen synthase. At the same time, there was more lactate and greater CO_2 production in Kir6.2$^{-/-}$ FDB, possibly due to the slow recovery of unstimulated force and thus unstimulated Ca^{2+}. It is possible the increase in catabolism during recovery in Kir6.2$^{-/-}$ FDB is due to the greater activation of AMPK during fatigue or from the higher $[Ca^{2+}]_i$ during recovery, as unstimulated force/Ca^{2+} remains at 4% of maximal tetanic force, compared to no

unstimulated force in wild type FDB following recovery.

CARBOHYDRATE METABOLISM AND ENERGY BALANCE

The most important aspect of this study was to determine how many glucosyl units from glycogen and extracellular glucose enters glycolysis, how much ends up as lactate, how much is oxidized and how much ATP is produced.

The sources of glucosyl units for wild type and Kir6.2$^{-/-}$ FDB are depicted in Figure 4-1A. There was no difference in the amount of usable glucose between wild type and Kir6.2$^{-/-}$ FDB. Both predominantly relied upon glycogen, being 87 and 81% of fuel sources in wild type and Kir6.2$^{-/-}$, respectively. The use of glycogen primarily as a fuel source is as expected, as the length of the fatigue period may not be long enough to stimulate GLUT4 to the cell membrane and thus activate glucose transport to its maximum.

Figure 4-1B shows the end metabolites produced during fatigue. For both wild type and Kir6.2$^{-/-}$ FDB, lactate is produced to a large extent, signifying that glycolysis was an energy pathway relied heavily upon during the fatigue period. This is as expected, considering the high contraction rate of one tetanus/sec. As previously discussed, Kir6.2$^{-/-}$ FDB had a larger proportion of the metabolites as CO_2, reflective of greater glucose oxidation. The "unexplained" portion represents the metabolic intermediates calculated during fatigue, and interestingly, there were no differences between wild type and Kir6.2$^{-/-}$ FDB.

Fig 4-1C represents the calculated ATP production in wild type and Kir6.2$^{-/-}$ FDB after 180 sec of fatigue. ATP production was calculated as follows: 2 ATP from glucose to lactate * amount coming from extracellular glucose; 3 ATP from glucose to lactate * amount coming from glycogen; 36 ATP per glucose to CO_2 * amount coming from

extracellular glucose; and 39 ATP per glucose to CO_2 coming from glycogen. Kir6.2$^{-/-}$ FDB generated 2.7-fold more ATP compared to wild type FDB (Fig 4-1C). In wild type FDB, the majority of ATP came from the degradation of PCr as well as glucose broken down to lactate, with very little coming from endogenous ATP. In Kir6.2$^{-/-}$ FDB, the amount of ATP produced from PCr breakdown and glycolytic breakdown was similar to that of wild type. However, ATP generation from the oxidation of glucose to CO_2 was greater in Kir6.2$^{-/-}$ FDB. This accounted for the majority of ATP production, which was 401 ATP μmole/g dry weight compared to only 154 μmole/g dry weight in wild type FDB. Kir6.2$^{-/-}$ FDB produce more ATP mainly through the oxidation of glucose, however this is still not sufficient to maintain normal ATP levels since they are significantly less than that of wild type FDB (Fig 1-1). Considering the increase in energy demand during 60 to 180 sec of fatigue in Kir6.2$^{-/-}$ FDB, and that ATP levels cannot be sustained, there must be a metabolic dysfunction as a result of the lack of K_{ATP} channel activity during fatigue.

FIGURE 4-1

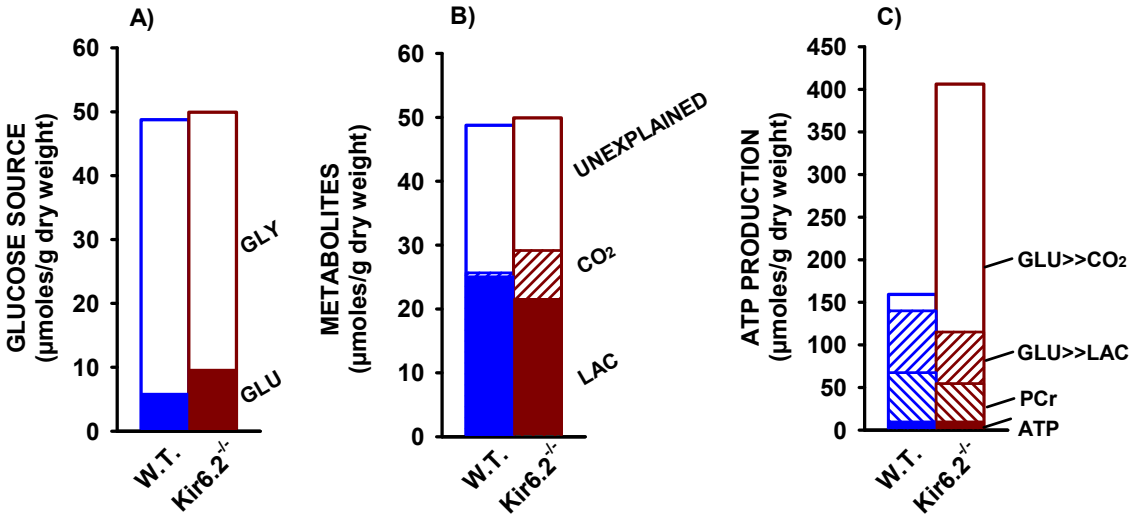

Figure 4-1. Compared to wild type FDB, the capacity for ATP production during fatigue was much greater in Kir6.2$^{-/-}$ FDB and was accomplished by oxidizing a greater amount of glucose to CO_2. ATP was calculated as follows: 2 ATP/lactate from extracellular glucose and 3 ATP/lactate from the breakdown of glycogen; 36 ATP/CO_2 from extracellular glucose and 39 ATP/CO_2 from the breakdown of glycogen.

Conclusion

In conclusion, Kir6.2$^{-/-}$ FDB demonstrate an initial increased ability to breakdown glycogen and to transport glucose during the first 60 and 180 sec of fatigue to meet the high energy demand as a result of increased unstimulated force and calcium. Kir6.2$^{-/-}$ FDB also oxidize more glucose during that time, allowing for greater ATP production. However this initial greater capacity to mobilize glycogen and extracellular glucose in Kir6.2$^{-/-}$ appeared to become impaired during the last 120 sec of fatigue; the difference in glycogen breakdown between wild type and Kir6.2$^{-/-}$ FDB disappeared and glucose oxidation no longer increased from 60 sec to 180 sec. So while Kir6.2$^{-/-}$ FDB generate more ATP, it appears insufficient to allow recovery in ATP as is observed in wild type FDB (Fig 1-1). Taken together, the results from this study show that muscle lacking functional K_{ATP} channels have an impairment in energy metabolism, consistent with the notion that the K_{ATP} channel is a crucial component in the process of fatigue.

CHAPTER 5

REFERENCE LIST

Andrews MAW, Godt RE and Nosek TM. Influence of physiological L(+)-lactate concentrations on contractility of skinned striated muscle fibers of rabbit. J Appl Physiol 80: 2060-2065, 1996.

Antcliff JF, Haider S, Proks P, Sansom MSP and Ashcroft FM. Functional analysis of a structural model of the ATP-binding site of the K_{ATP} channel Kir6.2 subunit. EMBO J 24: 229-239, 2005.

Babij P, Matthew SM and Rennie MJ. Changes in blood ammonia, lactate and amino acids in relation to workload during bicycle ergometer exercise in man. Eur J Appl Physiol 50: 405-411, 1983.

Balsom PD, Soderlund K, Sjodin B and Ekblom B. Skeletal muscle metabolism during short duration high-intensity exercise: influence of creatine supplementation. Acta Physiol Scand 154: 303-310, 1995.

Barrett-Jolley R, Comtois A, Davies NW, Stanfield PR and Standen NB. Effect of adenosine and intracellular GTP on K_{ATP} channels of mammalian skeletal muscle. J Membr Biol 152: 111-116, 1996.

Baukrowitz T, Schulte U, Oliver D, Herlitze S, Krauter T, Tucker SJ, Ruppersberg

JP and Fakler B. PIP2 and PIP as determinants for ATP inhibition of KATP channels. Science 282: 1141-1144, 1998.

Benkhalti, M. The effect of the KATP channel on energy metabolism in skeletal muscle during fatigue. M.Sc. Thesis. Univerwsity of Ottawa, Canada. 2009.

Bennetts B, Parker MW and Cromer BA. Inhibition of skeletal muscle ClC-1 chloride channels by low intracellular pH and ATP. J Biol Chem 282: 32780-32791, 2007.

Bennetts B, Rychkov GY, Ng H-L, Morton CJ, Stapleton D, Parker MW and Cromer BA. Cytoplasmic ATP-sensing domains regulate gating of skeletal muscle ClC-1 chloride channels. J Biol Chem 280: 32452-32458, 2005.

Bonen A, Dyck DJ, Ibrahami A and Abumrad NA. Muscle contractile activity increases fatty acid metabolism and transport and FAT/CD36. Am J Physiol Endocrinol Metab 276: E642-E649, 1999.

Bottinelli R, Schiaffino S and Reggiani C. Force-velocity relations and myosin heavy chain isoform compositions of skinned fibres from rat skeletal muscle. J Physiol (Lond) 437: 655-672, 1991.

Brooke MH, Choksi R and Kaiser KK. Inosine monophosphate production is proportional to muscle force in vitro. Neurology 36: 288-291, 1986.

Brotto MA, Biesiadecki BJ, Brotto LS, Nosek TM and Jin J-P. Coupled expression of troponin T and troponin I isoforms in single skeletal muscle fibers correlates with contractility. Am J Physiol 290: C567-C576, 2006.

Bruton JD, Lännergren J and Westerblad H. Effects of CO_2-induced acidification on the fatigue resistance of single mouse muscle fibers at 28°C. J Appl Physiol 85: 478-483, 1998.

Campbell-O'Sullivan SP, Constantin-Teodosiu D, Peirce N and Greenhaff PL. Low intensity exercise in humans accelerates mitochondrial ATP production and pulmonary oxygen kinetics during subsequent more intense exercise. J Physiol (Lond) 583: 931-939, 2002.

Chahine M, Bennett PB, George Jr. AL and Horn R. Functional expression and properties of the human skeletal muscle sodium channel. Pflugers Arch 427: 136-142, 1994.

Chesley A, Howlett RA, Heigenhauser GJF, Hultman E and Spriet LL. Regulation of muscle glycogenolytic flux during intense aerobic exercise after caffeine ingestion. Am J Physiol Regul Integr Comp Physiol 275: R595-R603, 1998.

Chin ER and Allen DG. Effects of reduced muscle glycogen concentration on force, Ca^{2+} release and contractile protein function in intact mouse skeletal muscle. J Physiol (Lond) 498: 17-29, 1997.

Cifelli C, Boudreault L, Gong B, Bercier JP and Renaud JM. Contractile dysfunctions in K_{ATP} channel deficient mouse FDB during fatigue involve Ca^{2+} influx through L-type Ca^{2+} channels. Exp Physiol 93: 1126-1138, 2008.

Cifelli C, Bourassa F, Gariépy L, Banas K, Benkhalti M and Renaud JM. K_{ATP} channel deficiency in mouse FDB causes fiber damage and impairs Ca^{2+} release and force development during fatigue in vitro . J Physiol (Lond) 582: 843-857, 2007.

Coetzee WA. Regulation of ATP sensitive potassium channel of isolated guinea pig ventricular myocytes by sarcolemmal monocarboxylate transport. Cardiovasc Res 26: 1077-1086, 1992.

Cook DL and Hales CN. Intracellular ATP directly blocks K^+ channels in pancreatic ß-cells. Nature 311: 271-273, 1984.

Cooke R, Franks K, Luciani GB and Pate E. The inhibition of rabbit skeletal muscle contraction by hydrogen ions and phosphate. J Physiol (Lond) 395: 77-97, 1988.

Davies NW, Standen NB and Stanfield PR. The effect of intracellular pH on ATP-dependent potassium channels of frog skeletal muscle. J Physiol (Lond) 445: 549-568, 1992.

de Paoli FV, Overgaard K, Pedersen TH and Nielsen OB. Additive protective effects of the addition of lactic acid and adrenaline on excitability and force in isolated rat skeletal muscle depreseed by elevated extracellular K^+. J Physiol (Lond) 581: 829-839, 2007.

Debold EP, Romatowski J and Fitts RH. The depressive effect of P_i on the force-pCa relationship in skinned single muscle fibers is temperature dependent. Am J Physiol 290: C1041-C1050, 2006.

Decking UKM, Reffelmann T and Kammermeier H. Hypoxia-induced activation of K_{ATP} channels limits energy depletion in the guinea pig heart. Am J Physiol Heart Circ Physiol 269: H734-H742, 1995.

Dudley GA and Terjung RL. Influence of acidosis on AMP deaminase activity in contracting fast-twitch muscle. Am J Physiol Cell Physiol 248: C43-C50, 1985.

Febbraio MA and Dancey J. Skeletal muscle energy metabolism during prolonged, fatiguing exercise. J Appl Physiol 87: 2341-2347, 1999.

Friden J, Seger J and Ekblom B. Topographical localization of muscle glycogen: an ultrahistochemical study in the human vastus lateralis. Acta Physiol Scand 135: 381-391, 1989.

Gandevia SC. Neural control in human muscle fatigue: changes in muscle

afferents, motoneurones and motor cortical drive. Acta Physiol Scand 162: 275-283, 1998.

Gibbs CL. Comparative muscle energetics and the cost of activation. Proc Austr Physiol Pharmac Soc 18: 115-123, 1987.

Godt RE and Nosek TM. Changes of intracellular milieu with fatigue or hypoxia depress contraction of skinned rabbit skeletal and cardiac muscle. J Physiol (Lond) 412: 155-180, 1989.

Gong B, Legault D, Miki T, Seino S and Renaud JM. K_{ATP} channels depress force by reducing action potential amplitude in mouse EDL and soleus. Am J Physiol Cell Physiol 285: C1464-C1474, 2003.

Graham TE, Yuan Z, Hill AK and Wilson RJ. The regulation of muscle glycogen: the granule and its proteins. Acta Physiol 199: 489-498, 2010.

Gramolini A and Renaud JM. Blocking ATP-sensitive K^+ channel during metabolic inhibition impairs muscle contractility. Am J Physiol Cell Physiol 41: C936-C946, 1997.

Gray.S.R., Soderlund K, Watson M and Ferguson RA. Skeletal muscle ATP turnover and single fibre ATP and PCr content during intense exercise at different muscle temperatures in humans. Pflugers Arch 462: 885-893, 2011.

Greaser ML and Gergely J. Purification and properties of the components from troponin. J Biol Chem 248: 2125-2133, 1973.

Green HJ, Duhamel TA, Smith IC, Rich SM, Thomas MM, Ouyang J and Yau JE. Muscle metabolic, enzymatic and transporter responses to a session of prolonged cycling. Eur J Appl Physiol 111: 827-837, 2011.

Greenhaff PL, Nevill ME, Soderlund K, Bodin K, Boobis L, Williams C and Hultman E. The metabolic responses of human type I and II muscle fibres during maximal treadmill sprinting. J Physiol (Lond) 478: 149-155, 1994.

Gumina RJ, Pucar D, Bast P, Hodgson DM, Kurtz CE, Dzeja PP, Miki T, Seino S and Terzic A. Knockout of Kir6.2 negates ischemic preconditioning-induced protection of myocardial energetics. Am J Physiol 284: H2106-H2113, 2003.

Han J, So I, Kim E-Y and Earm YE. ATP-sensitive potassium channels are modulated by intracellular lactate in rabbit ventricular myocytes. Pflugers Arch 425: 546-548, 1993.

Hancock CR, Jansson E and Terjung RL. Contraction-mediated phosphorylation of AMPK is lower in skeletal muscle of adenylate kinase-deficient mice. J Appl Physiol 100: 406-413, 2006.

Ho K, Nichols CG, Lederer WJ, Lytton J, Vassilev PM, Kanazirska MV and

Hebert SC. Cloning and expression of an inwardly rectifying ATP-regulated potassium channel. Nature 362: 31-38, 1993.

Houdusse A, Love ML, Dominguez R, Grabarek Z and Cohen C. Structures of four Ca^{2+}-bound troponin C at 2.0A resolution: further insights into the Ca2+-switch in the calmodulin superfamily. Structure 5: 1695-1711, 1997.

Howlett RA, Parolin ML, Dyck DJ, Hultman E, Jones NL, Heigenhauser GJF and Spriet LL. Regulation of skeletal muscle glycogen phosphorylase and PDH at varying exercise power outputs. Am J Physiol Regul Integr Comp Physiol 275: R418-R425, 1998.

Hultman E and Sjoholm H. Energy metabolism and contraction force of human skeletal muscle in situ during electrical stimulation. J Physiol (Lond) 345: 525-532, 1983.

Ihlemann J, Ploug T, Hellsten Y and Galbo H. Effect of stimulation frequency on contraction-induced glucose transport in rat skeletal muscle. Am J Physiol Endocrinol Metab 279: E862-E867, 2000.

Jensen TE, Rose AJ, Jorgensen SB, Brandt N, Schjerling P, Wojitaszewski JFP and Richter EA. Possible CaMKK-dependent regulation of AMPK phosphorylation and glucose uptake at the onset of mild tetanic skeletal muscle contraction. Am J Physiol Endocrinol Metab 292: E1308-E1317, 2007.

Jin J-P and Chong SM. Localization of the two tropomyosin-binding sites of troponin T. Arch Biochem Biophys 500: 144-150, 2010.

Jones NL, McCartney N, Graham TE, Spriet LL, Kowalchuk JM, Heigenhauser GJF and Sutton JR. Muscle performance and metabolism in maximal isokinetic cycling at slow and fast speeds. J Appl Physiol 59: 132-136, 1985.

Kane GC, Behfar A, Yamada S, Perez-Terzic C, O'Cochlain F, Reyes S, Dzeja PP, Miki T, Seino S and Terzic A. ATP-sensitive K^+ channel knockout compromises the metabolic benefit of exercise training, resulting in cardiac deficits. Diabetes 53: S169-S175, 2004.

Karlsson J and Saltin B. Lactate, ATP, and CP in working muscles during exhaustive exercise in man. J Appl Physiol 29: 598-602, 1970.

Kentish JC. The effects of inorganic phosphate and creatine phosphate on force production in skinned muscles from rat ventricle. J Physiol (Lond) 370: 585-604, 1986.

Keung EC and Li Q. Lactate activates ATP-sensitive potassium channels in guinea pig ventricular myocytes. J Clin Invest 88: 1772-1777, 1991.

Kiilerich K, Birk JB, Damsgaard R, Wojtaszewski JFP and Pilegaard H. Regulation of PDH in human arm and leg muscles at rest and during intense

exercise. Am J Physiol Endocrinol Metab 294: E36-E42, 2008.

Kleppisch T and Nelson T. Adenosine activates ATP-sensitive potassium channels in arterial myocytes via A2 receptors and cAMP-dependent protein kinase. Proc Natl Acad Sci 92: 12441-12445, 1995.

Krause E and Wegener G. Exercise and recovery in frog muscle: metabolism of PCr, adenine nucleotides, and related compounds. Am J Physiol Regul Integr Comp Physiol 270: R811-R820, 1996.

Kushmerick MJ, Larson RE and Davies RE. The chemical energetics of muscle contraction. I. Activation heat, heat of shortening and ATP utilization for activation-relaxation processes. Proc R Soc Lond B 174: 293-313, 1969.

Kushmerick MJ, Moerland TS and Wiseman RW. Mammalian skeletal muscle fibers distinguished by contents of phosphocreatine, ATP, and P_i. Proc Natl Acad Sci USA 89: 7521-7525, 1992.

Lederer WJ and Nichols CG. Nucleotide modulation of the activity of rat heart ATP-sensitive K^+ channels in isolated membrane patches. J Physiol (Lond) 419: 193-211, 1989.

Li, Z. The reationship between KATP channels and energy state in skeletal muscle during fatigue development. M.Sc. Thesis. University of Ottawa, Canada, 2007.

Lindinger MI, Heigenhauser GJF and Spriet LL. Effects of alkalosis on muscle ions at rest and with intense exercise. Can J Physiol Pharmacol 68: 820-829, 1990.

MacIntosh BR and Shahi MRS. A peripheral governor regulates muscle contraction. Appl Physiol Nutr Metab 36: 1-11, 2011.

Matar W, Nosek TM, Wong D and Renaud JM. Pinacidil suppresses contractility and preserves energy but glibenclamide has no effect during fatigue in skeletal muscle. Am J Physiol 278: C404-C416, 2000.

McCartney N, Spriet LL, Heigenhauser GJF, Kowalchuk JM, Sutton JR and Jones NL. Muscle power and metabolism in maximal intermittent exercise. J Appl Physiol 60: 1164-1169, 1986.

McGee SL and Hargreaves M. AMPK-mediated regulation of transcription in skeletal muscle. Clin Sci 118: 507-518, 2010.

McKenna MJ, Bangsbo J and Renaud JM. Muscle $K^{+,}$ Na^{+}, and Cl^{-} disturbances and Na+-K+ pump inactivation: implications for fatigue. J Appl Physiol 104: 288-295, 2008.

Meisheri KD, Fosset M, Humphrey SM and Lazdunski M. Receptor binding characterization in kidney membrane of [3H]U-37883, a novel ATP-sensitive K^{+} channel blocker with diuretic/natriuretic properties. Mol Pharmacol 47: 155-163,

1995.

Mercier P, Ferguson R, Irving M, Corrie J, Trentham D and Sykes BD. NMR structure of a bifunctional rhodamine labeled N-domain of troponin C complexed with the regulatory "switch" peptide from troponin I: implications for in situ flourescence studies in muscle fibers. Biochem J 42: 4333-4348, 2003.

Meyer RA, Brown TR, Krilowicz BL and Kushmerik MJ. Phosphagen and intracellular pH changes during contraction of creatine-depleted rat muscle. Am J Physiol Cell Physiol 250: C264-C274, 1986.

Miki T, Liss B, Minami K, Shiuchi T, Saraya A, Kashihara Y, Horiuchi M, Ashcroft FM, Minokoshi Y, Roeper J and Seino S. ATP-sensitive K^+ channels in the hypothalamus are essential for the maintenance of glucose homeostasis. Nature Neurosicence 4: 507-512, 2001.

Miki T, Minami K, Zhang L, Morita M, Gonoi T, Shiuchi T, Minokoshi Y, Renaud JM and Seino S. ATP-sensitive potassium channels participate in glucose uptake in skeletal muscle and adipose tissue. Am J Physiol Endocrinol Metab 283: E1178-E1184, 2002.

Miki T, Nagashima H, Tashiro F, Kotake K, Yoshitomi H, Tamamoto A, Gonoi T, Iwanaga T, Miyazaki J-I and Seino S. Defective insulin secretion and enhanced insulin action in K_{ATP} channel-deficient mice. Proc Natl Acad Sci 95: 10402-

10406, 1998.

Minami K, Morita M, Saraya A, Yano H, Terauchi Y, Miki T, Kuriyama T, Kadowaki T and Seino S. ATP-sensitive K^+ channel-mediated glucose uptake is independent of IRS-1/phosphatidylinositol 3-kinase signaling. Am J Physiol Endocrinol Metab 285: E1289-E1296, 2003.

Mu J, Brozinick JT, Valladares O, Bucan M and Bimbaum MJ. A role for AMP-activated protein kinase in contraction- and hypoxia-regulated glucose transport in skeletal muscle. Molecular Cell 7: 1085-1094, 2001.

Murphy BJ and Tuana BS. Calcium ions inhibit the allosteric interaction between the dihydropyridine and phenylalkylamine binding site on the voltage-gated calcium channel in heart sarcolemma but not in skeletal muscle transverse tubules. Can J Physiol Pharmacol 68: 1389-1395, 1990.

Nakai JSN, Rando TA, Allen PD and Beam KG. Two regions of the ryanodine receptor involved in coupling with L-type Ca^{2+} channels. J Biol Chem 273: 13403-13406, 1998.

Nichols CG. K_{ATP} channels as molecular sensors of cellular metabolism. Nature 440: 470-476, 2006.

Nielsen J, Schroder HD, Rix CG and Orthenblad N. Distinct effects of subcellular

glycogen localization on tetanic relaxation time and endurance in mechanically skinned rat skeletal muscle fibres. J Physiol (Lond) 587: 3679-3690, 2009.

Nielsen JJ, Holmber HC, Schroder HD, Saltin B and Orthenblad N. Human skeletal muscle glycogen utilization in exhaustive exercise: role of subcellular localization and fibre type. J Physiol (Lond) 589: 2871-2885, 2011.

Nielsen JJ, Kristensen M, Hellsten Y, Bangsbo J and Juel C. Localization and function of ATP-sensitive potassium channels in human skeletal muscle. Am J Physiol 284: R558-R563, 2003.

Noma A. ATP-regulated K^+ channels in cardiac muscle. Nature 305: 147-148, 1983.

Odland R, Howlett RA, Heigenhauser GJF, Hultman E and Spriet LL. Skeletal muscle malonyl-CoA content at the onset of exercise at varying power outputs in humans. Am J Physiol Endocrinol Metab 274: E1080-E1085, 1998.

Ortenblad N, Macdonald WA and Sahlin K. Glycolysis in contracting rat skeletal muscle is controlled by factors related to energy state. Biochem J 420: 161-168, 2009.

Ørtenblad N and Stephenson DG. A novel signalling pathway originating in mitochondria modulates rat skeletal muscle membrane excitability. J Physiol

(Lond) 548: 139-145, 2003.

Parmacek MS, Bengur AR, Vora AJ and Leiden JM. The structure and regulation of expression of the murine fast skeletal troponin C gene. Identification of a developmentally regulated, muscle-specific transcriptional enhancer. J Biol Chem 265: 15970-15976, 1990.

. Parmacek MS and Leiden JM. Structure and expression of the murine slow/cardiac troponin C gene. J Biol Chem 264: 13217-13225, 1989.

Pate E, Bhimani M, Franks-Skiba K and Cooke R. Reduced effect of pH on skinned rabbit psoas muscle mechanics at high temperatures: implications for fatigue. J Physiol (Lond) 486: 689-694, 1995.

Pedersen TH, Macdonald WA, de Paoli FV, Gurung.I.S. and Nielsen OB. Comparison of regulated passive membrane conductance in action potential-firing fast- and slow-twitch muscle. J Gen Physiol 134: 323-337, 2009.

Piao, Cui, Xu, Mao, Rojas, Wang, Abdulkadir, Li, Wu J and Jiang C. Requirement of multiple protein domains and residues for gating K(ATP) channels by intracellular pH. J Biol Chem 276: 36673-36680, 2001.

Putnam RW. The role of lactic acid accumulation in muscle fatigue of two species of anurans, Xenopus laevis and Rana pipiens. J Exp Biol 82: 35-51, 1979.

Rall JA. Energetic aspects of skeletal muscle contraction: implications of fiber types. Exercise Sport Science Review 13: 33-74, 1985.

Raney MA and Turcotte LP. Evidence for the involvement of CaMKII and AMPK in Ca^{2+}-dependent signaling pathways regulating FA uptake and oxidation in contracting rodent muscle. J Appl Physiol 104: 1366-1373, 2008.

Reiser PJ, Moss RL, Giulian GG and Greaser ML. Shortening velocity in single fibers from adult rabbit soleus muscles is correlated with myosin heavy chain composition. J Biol Chem 260: 9077-9080, 1985.

Ren J-M, Broberg S, Sahlin K and Hultman E. Influence of reduced glycogen level on glycogenolysis during short-term stimulation in man. Acta Physiol Scand 139: 467-474, 1990.

Sahlin K, Broberg S and Ren J-M. Formation of inosine monophosphate (IMP) in human skeletal muscle during incremental dynamic exercise. Acta Physiol Scand 136: 193-198, 1989.

Sahlin K and Harris RC. The creatine kinase reaction: a simple reaction with functional complexity. Amino Acids 40: 1363-1367, 2011.

Sahlin K and Katz A. Hypoxaemia increases the accumulation of inosine monophosphate (IMP) in human skeletal muscle during submaximal exercise.

Acta Physiol Scand 136: 199-203, 1989.

Sahlin K, Soderlund K, Tonkonogi M and Hirakoba K. Phosphocreatine content in single fibers of human muscle after sustained submaximal exercise. Am J Physiol Cell Physiol 273: C172-C178, 1997.

Sato T, Wu B, Nakamura S, Kiyosue T and Arita M. Cibenzoline inhibits diazoxide- and 2,4-dinitrophenol-activated ATP-sensitive K^+ channels in guinea-pig ventricular cells. Br J Pharmacol 108: 549-556, 1993.

Shyng SL, Cukras CA, Harwood J and Nichols CG. Structural determinants of PIP(2) regulation of inward rectifier K(ATP) channels. J Gen Physiol 116: 599-607, 2000.

Shyng SL, Ferrigni T and Nichols CG. Regulation of K_{ATP} channel activity by diazoxide and MgADP: Distinct functions of the two nucleotide binding folds of the sulfonylurea receptor. J Gen Physiol 110: 643-654, 1997.

Shyng SL and Nichols CG. Membrane phospholipid control of nucleotide sensitivity of KATP channels. Science 282: 1138-1141, 1998.

Slupsky C and Sykes BD. NMR solution structure of calcium-saturated skeletal muscle troponin C. Biochem J 34: 15953-15964, 1995.

Spriet LL. ATP utilization and provision in fast-twitch skeletal muscle during tetanic contractions. Am J Physiol Endocrinol Metab 257: E595-E605, 1989.

Spriet LL. Anaerobic ATP provision, glycogenolysis and glycolysis in rat slow-twitch muscle during tetanic contractions. Pflugers Arch 417: 278-284, 1990.

Spriet LL. Phosphofructokinase activity and acidosis during short-term tetanic contractions. Can J Physiol Pharmacol 69: 298-304, 1991.

Spriet LL, Matsos CG, Peters SJ, Heigenhauser GJF and Jones NL. Muscle metabolism and performance in perfused rat hindquarter during heavy exercise. Am J Physiol Cell Physiol 248: C109-C118, 1985.

Spriet LL, Soderlund K, Bergström M and Hultman E. Anaerobic energy release in skeletal muscle during electrical stimulation in men. J Appl Physiol 62: 611-615, 1987.

Spruce AE, Standen NB and Stanfield PR. Voltage dependent ATP-sensitive potassium channels of skeletal muscle membrane. Nature 316: 736-738, 1985.

Standen NB, Pettit AI, Davies NW and Stanfield PR. Activation of ATP-dependent K^+ currents in intact skeletal muscle fibres by reduced intracellular pH. Proc R Soc Lond B 247: 195-198, 1992.

Staron RS. Human skeletal muscle fiber types: delineation, development, and distribution. Can J Appl Physiol 22: 307-327, 1997.

Suzuki M, Sasaki N, Miki T, Sakamoto N, Ohmoto-Sekine Y, Tamagawa M, Seino S, Marban E and Nakaya H. Role of sarcolemmal KATP channels in cardioprotection against ischemia/reperfusion injury in mice. J Clin Invest 109: 509-516, 2002.

Talanian JL, Holloway GP, Snook LA, Heigenhauser GJF, Bonen A and Spriet LL. Exercise training increases sarcolemmal and mitochondrial fatty acid transport proteins in human skeletal muscle. Am J Physiol Endocrinol Metab 299: E180-E188, 2010.

Talanian JL, Tunstall RJ, Watt MJ, Duong M, Perry CGR, Steinberg GR, Kemp GJ, Heigenhauser GJF and Spriet LL. Adrenergic regulation of HSL serine phosphorylation and activity in human skeletal muscle during the onset of exercise. Am J Physiol Regul Integr Comp Physiol 291: R1094-R1099, 2006.

Tanabe T, Beam KG, Adams BA, Niidome T and Numa S. Regions of the skeletal muscle dihydropyridine receptor critical for excitation-contraction coupling. Nature 346: 567-569, 1990.

Tanabe T, Mikami A, Numa S and Beam KG. Cardiac-type excitation-contraction coupling in dysgenic skeletal muscle injected with cardiac dihydropyridine

receptor cDNA. Nature 344: 451-453, 1990.

Thabet M, Miki T, Seino S and Renaud JM. Treadmill running causes significant damage in skeletal of muscle K_{ATP} channel deficient mice. Physiol Gen 22: 204-212, 2005.

Thong FSL, Bilan PJ and Klip A. The Rab GTPase-activating protein AS160 integrates Akt, protein kinase C, and AMP-activated protein kinase signals regulating GLUT4 traffic. Diabetes 56: 414-423, 2007.

Tricarico D, Capriulo R and Camerino DC. Insulin modulation of ATP-sensitive K^+ channel of rat skeletal muscle is impaired in the hypokalaemic state. Pflugers Arch 437: 235-240, 1999.

Tsintzas K, Williams C, Constantin-Teodosiu D, Hultman E, Boobis L, Clarys P and Greenhaff PL. Phosphocreatine degradation in type I and type II muscle fibres during submaximal exercise in man: effect of carbohydrate ingestion. J Physiol (Lond) 537: 305-311, 2001.

Tucker SJ, Gribble FM, Proks P, Trapp S, Ryder TJ, Haug T, Reimann F and Ashcroft FM. Molecular determinants of K_{ATP} channel inhibition by ATP. EMBO J 17: 3290-3296, 1998.

Tucker SJ, Gribble FM, Zhao C, Trapp S and Ashcroft FM. Truncation of Kir6.2

produces ATP-sensitive K^+ channels in the absence of the sulphonylurea receptor. Nature 387: 179-183, 1997.

Vinogradova M, Stone D, Malanina G, Karatzaferi C, Cooke R, Mendelson R and Fletterick R. Ca^{2+}-regulated structural changes in troponin. Proc Natl Acad Sci 102: 5038-5043, 2005.

Vivaudou MB, Arnoult C and Villaz M. Skeletal muscle ATP-sensitive K^+ channels recorded from sarcolemmal blebs of split fibers: ATP inhibition is reduced by magnesium and ADP. J Membr Biol 122: 165-175, 1991.

Wall BT, Stephens FB, Marimuthu K, Constantin-Teodosiu D and Greenhaff PL. Acute pantothenic acid and cysteine supplementation does not affect muscle co-enzyme A content, fuel selection or exercise performance in healthy humans. J Appl Physiol 2011.

Welsh DG and Lindinger MI. Metabolite accumulation increases adenine nucleotide degradation and decreases glycogenolysis in ischaemic rat skeletal muscle. Acta Physiol Scand 161: 203-210, 1997.

Wendt IR and Fitts RH. Energy production of rat extensor digitorum longus muscle. Am J Physiol 224: 1081-1086, 1973.

Westerblad H and Allen DG. Changes of myoplasmic calcium concentration

during fatigue in single mouse muscle fibers. J Gen Physiol 98: 615-635, 1991.

Westerblad H and Allen DG. Changes of intracellular pH due to repetitive stimulation of single fibres from mouse skeletal muscle. J Physiol (Lond) 449: 49-71, 1992.

Westerblad H, Lee JA, Lamb AG, Bolsover SR and Allen DG. Spatial gradients of intracellular calcium in skeletal muscle during fatigue. Pflugers Arch 415: 734-740, 1990.

Westerblad H, Lee JA, Lännergren J and Allen DG. Cellular mechanisms of fatigue in skeletal muscle. Am J Physiol Cell Physiol 261: C195-C209, 1991.

Widrick JJ, Trappe SW, Costill DL and Fitts RH. Force-velocity and force-power properties of single muscle fibers from elite master runners and sedentary men. Am J Physiol Cell Physiol 271: C676-C683, 1996.

Wright DC, Geiger PC, Holloszy JO and Han DH. Contraction- and hypoxia-stimulated glucose transport is mediated by a Ca^{2+}-dependent mechanism in slow-twitch rat soleus muscle. Am J Physiol Endocrinol Metab 288: E1062-E1066, 2005.

Wright DC, Hucker KA, Holloszy JO and Han DH. Ca2+ and AMPK both mediate stimulation of glucose transport by muscle contractions. Diabetes 53:

330-335, 2004.

Wu K and Lytton J. Molecular cloning and quantification of sarcoplasmic reticulum Ca^{2+}-ATPase isoforms in rat muscles. Am J Physiol Cell Physiol 264: C333-C341, 1993.

Zhao S, Snow RJ, Stathis CG, Febbraio MA and Carey MF. Muscle adenine nucleotide metabolism during and in recovery from maximal exercise in humans. J Appl Physiol 88: 1513-1519, 2000.

APPENDIX 1

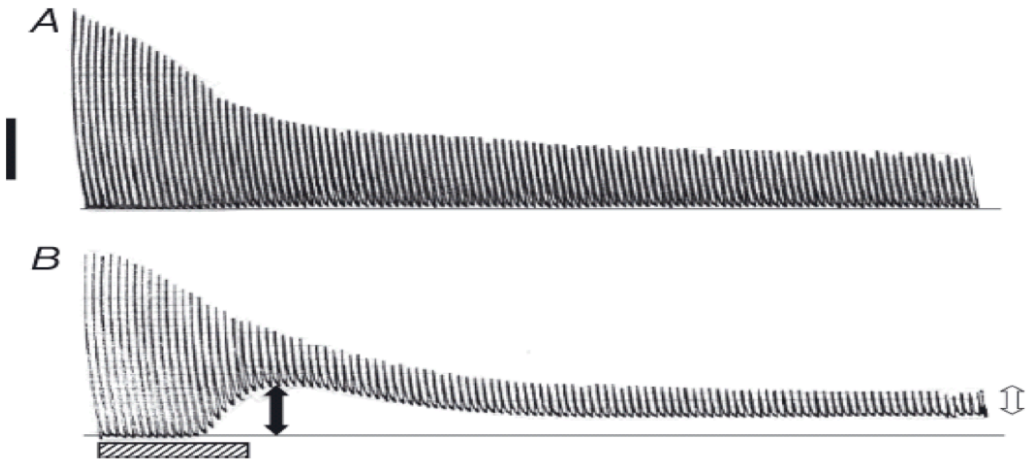

Appendix 1. Representative force traces for wild type FDB (A) and Kir6.2$^{-/-}$ FDB (B). Muscles were contracted once per sec for 180 sec. From Cifelli et al., 2007.